Environmental Science and Pollution Research
https://doi.org/10.1007/s11356-026-37880-z

RESEARCH ARTICLE

Production and characterization of iron oxide immobilized bioflocculants in the removal of *Microcystis aeruginosa* from freshwater ecosystems

Jayaprakash Arulraj[1] · Vino Udappusamy[2] · Priya Sundararajan[3] · Shalini Ganeshan[2] · Nirmal Kumar Ramasamy[2] · Revathy Soundararajan[1] · Embranahalli Mani Rajesh[1] · Gayathri Kaliyannan[4]

Received: 24 October 2025 / Accepted: 25 May 2026

Abstract

Harmful algal blooms (HABs) have significantly influenced water pollution and created negative impacts on biotic and abiotic ecosystems. *Microcystis aeruginosa* was found to be a major cyanobacterium that causes HABs in freshwater ecosystems. In order to remove HABs, a flocculation mechanism was adopted. As synthetic flocculants exhibit toxicity, microbial-based flocculants were used. Further, in this study, iron oxide (Fe_3O_4) nanoparticles were immobilized with bioflocculants to enhance the efficacy in removing HABs. Initially, the Fe_3O_4 immobilized bioflocculants were characterized based on UV–visible spectroscopy, FTIR, DLS, SEM, EDX, HR-TEM, XRD, and VSM analysis. Subsequently, *Microcystis aeruginosa* was cultivated in optimized conditions and its biomass was calculated. Further, about 96% of the flocculation of *Microcystis aeruginosa* was observed at optimum pH of 7, temperature of 37 °C, agitated rate of 120 rpm, and complete settling time of 60 min. Moreover, Fe_3O_4 immobilized bioflocculants could be used up to four times, which could help in reducing the treatment cost. Consequently, it was found that flocculation occurred through a bridging mechanism based on zeta potential analysis. Furthermore, a comparative analysis was performed to compare the efficacy of Fe_3O_4 immobilized bioflocculant with commercially available flocculants. It was revealed that Fe_3O_4 immobilized bioflocculant was more efficient than synthetic flocculants. Based on physicochemical parameters, water treated with Fe_3O_4 immobilized bioflocculants was found to be within the permissible limit of Indian Standards for drinking water. Hence, this method could be effectively used for drinking purposes. Further, the antimicrobial activity of Fe_3O_4 immobilized bioflocculants exhibited significant activity against water pathogens. Moreover, molecular docking studies revealed that the active compound Lidocaine of Fe_3O_4 immobilized bioflocculant showed effective binding at threonine-221 of the target with one hydrogen bond interaction. The results of this study suggest that Fe_3O_4 immobilized bioflocculants have potential for removing harmful algal blooms from freshwater ecosystems.

Keywords Harmful algal blooms · *Microcystis aeruginosa* · Bioflocculants · Iron oxide nanoparticles · Water purification · Molecular docking

Introduction

Freshwater ecosystems are important for maintaining the balance of life on Earth and provide a vital resource for drinking, aquaculture, agriculture, and industrial purposes. However, the increases in anthropogenic activities such as discharging sewage wastewater, industrial wastes, agriculture wastes, and fertilizers have led to a significant reduction in the availability of freshwater resources. These pollutants gradually increase the nutrient levels in freshwater bodies, accelerating eutrophication and aiding the excessive growth of harmful algal (cyanobacteria) blooms (Okaiyeto et al. 2016; Mushtaq et al. 2019; Kesheri et al. 2021, 2022).

Responsible Editor: Angeles Blanco

✉ Gayathri Kaliyannan
gayabio89@gmail.com

[1] Department of Microbiology, PSG College of Arts & Science, Coimbatore, Tamil Nadu 641014, India

[2] Department of Biotechnology, PSGR Krishnammal College for Women, Coimbatore, Tamil Nadu 641004, India

[3] Department of Microbiology, School of Life Sciences, Vels Institute of Science, Technology and Advanced Studies (VISTAS), Chennai, Tamil Nadu 600117, India

[4] Department of Biomaterials, SIMATS Deemed University Saveetha Dental College, Chennai, India

Published online: 04 June 2026

Among harmful algal blooms, the cyanobacteria species *Microcystis aeruginosa* is a major threat to water and aquatic animals. These algal blooms block sunlight to disturb photosynthesis and lead to oxygen depletion in aquatic animals, thereby affecting biodiversity. Moreover, *Microcystis aeruginosa* produces microcystin as a potent hepatotoxin that can result in major health risks to aquatic organisms, livestock, and humans (Zhang et al. 2022). Based on the severity of its negative impact on both biotic and abiotic processes in freshwater ecosystems, the effective control and removal of *Microcystis aeruginosa* are important for environmental safety. Several physical, chemical, and biological methods have been used for the removal of harmful algal blooms from freshwater. However, extensive use of chemicals like alum, ferric chloride, and polyacrylamide in the harmful algal removal is toxic to the environment. Also, these chemical treatments have a high capital cost, are non-biodegradable, and affect freshwater ecosystems (Khan et al. 2022; Zhang et al. 2022). These drawbacks limit their applicability, particularly in open water and large-scale operations.

Recent developments in sustainable water treatment have emphasized the use of cellulose-based bioflocculants as environmentally benign and efficient materials for cyanobacterial removal. Cellulose and its derivatives are biodegradable, non-toxic, and rich in hydroxyl (–OH) functional groups, which enable extensive hydrogen bonding interactions with extracellular polymeric substances (EPS), proteins, and polysaccharides present on the surface of *Microcystis aeruginosa*. These properties make cellulose-derived polymers particularly suitable for eco-friendly algal remediation applications. In particular, bioflocculants from microorganisms such as bacteria, fungi, and algae have shown promising potential due to their biodegradability, eco-friendliness, and non-toxicity (Agunbiade et al. 2018; Kurniawan et al. 2022). However, despite their advantages, individual bioflocculants may suffer from problems such as low efficiency and limited reusability under varying environmental conditions. To overcome these limitations and improve flocculation efficiency, recent developments have explored the immobilization of bioflocculants with nanoparticles.

Magnetic Fe_3O_4 nanoparticles have previously been reported as effective materials for algal harvesting due to their magnetic recoverability and adsorption capability. In such systems, algal removal is primarily governed by surface adsorption and magnetic separation. However, bare Fe_3O_4 nanoparticles often exhibit limited functional surface groups and may require higher dosages to achieve efficient flocculation. Recent studies have highlighted the effectiveness of cellulose-based bioflocculants for algal removal owing to their biodegradability and the abundance of hydroxyl and carboxyl functional groups capable of forming hydrogen bonds with algal cell surfaces. These polymeric materials enhance bridging interactions and improve floc stability. In the present study, the immobilization of a bioflocculant onto Fe_3O_4 nanoparticles combines the advantages of polymer-assisted flocculation with magnetic recoverability. This supported bioflocculant system provides enhanced surface functionality, improved interaction with algal extracellular polymeric substances (EPS), and reusability through magnetic separation, representing an advancement over systems employing Fe_3O_4 nanoparticles alone (Solomon et al. 2024; Jabbar et al. 2022; Ajith et al. 2021; Markeb et al. 2019).

The present study aims to develop and evaluate microbial bioflocculant-immobilized iron oxide nanoparticles for the effective removal of *Microcystis aeruginosa* from polluted water.

Materials and methods

Algae culture cultivation

The harmful algal-bloom-producing freshwater *Microcystis aeruginosa* NRMCF052 was obtained from Bharathidasan University (Tiruchirappalli, Tamil Nadu, India). Before the experiments, *Microcystis aeruginosa* was cultivated in 500 mL of BG-11 medium to enrich culture growth (Vergini et al. 2016). A pre-cultured *Microcystis aeruginosa* was grown in a 1 L photobioreactor under aseptic environmental conditions: pH 7, temperature 25 ± 2 °C, and light intensity of 3200 lx was provided on a 12:12 (light and dark) cycle. All experiments were performed in a sterile environment. The media, glassware, and apparatus were sterilized by autoclave at 15 lbs pressure for 30 min. The algae cultivation duration was 20 days, and the biomass concentration of *Microcystis aeruginosa* was evaluated every 24 h.

Synthesis and immobilization of bioflocculants in iron oxide nanoparticles

The magnetic iron oxide nanoparticles were synthesized using the co-precipitation method according to the procedure described by Markeb et al. 2019. Then, the bioflocculants obtained from *Bacillus subtilis* (Jayaprakash et al. 2023) were immobilized with iron oxide nanoparticles, based on the protocol mentioned by Idris and Suzana 2006. In this, calcium chloride was used as a cross-linking agent for the immobilization of bioflocculant in Fe_3O_4 nanoparticles.

Characterization of Fe_3O_4 nanoparticles and bioflocculant-immobilized Fe_3O_4 nanoparticles

UV–visible spectroscopy

The analysis of the absorption spectrum of Fe_3O_4 nanoparticles and bioflocculant-immobilized Fe_3O_4 nanoparticles

using an ultraviolet–visible spectrometer (Shimadzu, UV-1700 spectrophotometer, GRG-CATR, PSGR Krishnammal College for Women, Coimbatore, India) between a range of 200–800 nm, which is a common technique to characterize the optical properties of these nanoparticles (Khatun et al. 2022).

FTIR

The presence of functional groups in the Fe_3O_4 nanoparticle and bioflocculant-immobilized Fe_3O_4 nanoparticle was identified by Fourier transform infrared (FTIR, Shimadzu IRAffinity-1S model, PSGR Krishnammal College for Women, Coimbatore, India) spectroscopy. About 0.5 g of bioflocculant-immobilized iron oxide nanoparticles or iron oxide nanoparticles was mixed with 100 mg of KBr and pressed with a hydraulic pellet press that helps to create a thin layer of sample pellet. Then, the sample pellet was placed in the sample holder. It was then allowed to scan at a range of 4000–400 cm^{-1} (Manivasagan et al. 2015; Udappusamy et al. 2025).

SEM-EDAX

The morphological structure and elemental analysis of the Fe_3O_4 nanoparticle and bioflocculant-immobilized Fe_3O_4 nanoparticle were observed through a scanning electron microscope (SUPRA 55 VP-4132 and SIGMA-0261 (Carl Zeiss) equipped with EDS in Coimbatore Institute of Technology, Coimbatore, India). The sample was fixed onto adhesive tape and kept on a specimen holder. It was then quoted with Rock Spin Coder, and the respective morphology and elements were identified (Prodan et al. 2013; Udappusamy et al. 2025).

HR-TEM

The internal structure and size of Fe_3O_4 nanoparticles and Fe_3O_4 immobilized bioflocculant were detected by high-resolution transmission electron microscopy HR-TEM, with images captured at an accelerating voltage of 200 kV (JEOL 2100). Also, it gives direct information about lattice fringes and structure at the atomic level. The sample was prepared by placing a precise amount of the bioflocculant-immobilized iron oxide nanoparticles or iron oxide nanoparticles on a copper grid and allowing them to air dry before analysis. The HRTEM captured the internal structures and sizes of the iron oxide nanoparticles and bioflocculant-immobilized iron oxide nanoparticles (Stolyar et al. 2021).

XRD

X-ray diffraction is a technique used to study the crystallographic structure of materials. It can provide information about the lattice spacing, crystal orientation, and phase composition of free Fe_3O_4 nanoparticles and bioflocculant-immobilized Fe_3O_4 nanoparticles. The X-ray diffraction determined the nanoparticles' size (1 to 100 nm) and crystallographic structure using XRD, Empyrean, Malvern Panalytical, and 3rd generation (Fraga-Garcia et al. 2018).

Zeta potential

Zeta potential characterization plays a crucial role in understanding the surface charge and stability of bioflocculant-immobilized Fe_3O_4 nanoparticles. This zeta potential analyzer measures the electrostatic potential of the bioflocculant-immobilized Fe_3O_4 nanoparticles. Particles with higher absolute zeta potential values (positive or negative) tend to repulse each other to enhance aggregation and flocculation stability (Zetasizer—M3-PALS, Malvern Panalytical) (Abbasi et al. 2020; Govindhan et al. (2018).

Antibacterial activity

The antibacterial activity of the bioflocculant-immobilized Fe_3O_4 nanoparticles against pathogenic bacteria (*E. coli*, *Salmonella* sp., *Shigella* sp., and *Klebsiella* sp.) was evaluated using the well-diffusion method. Before the experiment, pure cultures of each pathogenic bacterium were subcultured onto nutrient broth and incubated at 35 °C on a rotary shaker (180 rpm). Therefore, nutrient agar plates were prepared, and wells were created on the agar using a gel puncture tool. Each bacterial strain was uniformly swabbed onto individual nutrient agar plates using sterile cotton. Followingly, different volumes of the bioflocculant-immobilized Fe_3O_4 nanoparticles (25 µL, 50 µL, 75 µL, and 100 µL) were inoculated into the separate wells on the all-nutrient agar plates. Afterwards, the different volumes of samples were loaded into the wells, and the plates were incubated at an appropriate temperature of 37 °C for 24 h. After incubation, nutrient agar plates were examined for inhibition zones around each well. These clear zones were measured using a zone-measuring scale, and distilled water was used as a control (Muthulakshmi et al. 2017).

Effect of Microcystis aeruginosa removal using Fe_3O_4 immobilized bioflocculant

The *Microcystis aeruginosa* flocculation experiments were performed in different conditions of dosage concentration,

pH, temperature, stirring speed, stirring time, and settling time. All experiments were performed in triplicate (Li et al. 2018).

Effect of dosage

Different dosage concentrations of 10 to 100 mg/L bioflocculant-immobilized Fe_3O_4 nanoparticles were used to evaluate the flocculation efficiency against *Microcystis aeruginosa* to find the optimal dosage level. All experiments were performed in triplicate (Li et al. 2018).

Effect of pH

The Fe_3O_4 immobilized bioflocculants' flocculation efficacy against *Microcystis aeruginosa* was tested at different pH levels of 2, 4, 6, 8, 10, and 12 to determine the bioflocculants' tolerance in acidic and alkaline conditions, altering the pH of *Microcystis aeruginosa* algal water by adding 1 N NaOH or HCl. All experiments were performed in triplicate (Li et al. 2018).

Effect of temperature

The flocculation efficiency of Fe_3O_4 immobilized bioflocculants at different temperatures ranging from 10 to 100 °C was determined to identify the temperature sensitivity of the bioflocculant *Microcystis aeruginosa* removal. Therefore, temperature can be altered by using temperature-controlled water baths, hot air ovens, and incubators. All experiments were performed in triplicate (Li et al. 2018).

Effect of stirring speed

The stirring speed of Fe_3O_4 immobilized bioflocculants in *Microcystis aeruginosa* removal in different mixing or stirring speeds impacts the flocculation process. Each sample's flocculation activity was determined at a different stirring speed from low to high (100 to 200 rpm) and can be achieved using a magnetic stirrer. All experiments were performed in triplicate (Li et al. 2018).

Effect of stirring time

The stirring time of Fe_3O_4 immobilized bioflocculants in *Microcystis aeruginosa* removal in different durations of stirring from 5 to 30 min influences the flocculation process and the subsequent removal of Microcystis cells from the water. Stirring times can vary from short to long and can be achieved using a magnetic stirrer. All experiments were performed in triplicate (Li et al. 2018).

Effect of settling time

Settling time is essential for achieving effective flocculation and removal of *Microcystis aeruginosa*. After stirring, the water samples were left undisturbed in conical flasks to allow the flocs to settle. After that, the water samples were analyzed at 5 min intervals to determine the remaining suspended particles (Li et al. 2018).

Microcystis aeruginosa removal and reusability of Fe_3O_4 immobilized bioflocculants

Based on the optimized conditions, the immobilized bioflocculant and *Microcystis aeruginosa* were incubated for 5 min. After 5 min, an external magnet was placed to separate the flocs from the water. The aliquots of the supernatant were taken and observed in UV–Visible spectrometry at 750 nm. Therefore, an uninoculated, immobilized bioflocculant water sample was used as a control for all experiments (OD_0). Following, *aeruginosa* removal was calculated according to the following equation described by Fraga-Garcia et al. 2018.

$$\text{Removal efficiency } (\%) = \left(1 - OD_1/OD_0\right) \times 100$$

where OD_1 corresponds to the absorbance of the bioflocculant-treated water sample.

For immobilized bioflocculant reuse, the *Microcystis aeruginosa* were separated from the flocs by changing pH with 1 N NaOH or HCl. Then, the *Microcystis aeruginosa* were filtered and the immobilized bioflocculant was collected for reuse. Therefore, the collected immobilized bioflocculant was resuspended to flocculate at optimal conditions for microalgae and separated again using an external magnet.

$$\text{Recovery efficiency and reusability } (\%) = OD_2/OD_0 \times 100$$

where OD_2 represents the final absorbance of the supernatants.

Flocculation mechanism

The zeta potentials of bioflocculant-immobilized Fe_3O_4 nanoparticles, *Microcystis aeruginosa*, and the mixture of immobilized bioflocculant and *Microcystis aeruginosa* were measured by a zeta potential analyzer (Zetasizer—M3-PALS, Malvern) to test flocculation mechanisms (Bisht and Lal 2019).

Evaluation of physicochemical and biological parameters

The bioflocculant-immobilized Fe_3O_4 nanoparticles were used to treat harmful algal water, and the water quality

before and after flocculation was evaluated. The physicochemical properties of the harmful algal, water color, odor, pH, TSS, TDS, turbidity, BOD, COD, total alkalinity, total hardness, calcium, magnesium, sodium carbonate, chloride, chlorine, nitrate nitrogen, fluoride, fecal coliform, *E. coli*, dissolved phosphate, sulfate, and sulfide, were analyzed as per Indian standards guidelines and procedures (Bureau of Indian Standards IS: 10500-2012) (Mallika et al. 2017).

Comparative efficacy of Fe_3O_4 immobilized bioflocculants with traditional flocculants

The purified bioflocculant and immobilized iron oxide nanoparticle harmful algae removal efficacy were compared with traditional flocculants of ferric chloride, alum, polyethyleneimine, and polyacrylamide. Based on Agunbiade et al. 2018, flocculation efficiency was compared with traditional flocculants. Each flocculant was prepared in a different concentration for the flocculation efficiency investigation to test against harmful algal water. Subsequently, control experiments were prepared without adding flocculants; distilled water was used instead of flocculants, and the flocculation efficacy was measured. The comparative studies on flocculating activity were measured as discussed earlier.

In silico analysis of molecular docking for identifying the interaction between Fe_3O_4 immobilized bioflocculants and Microcystis aeruginosa

Molecular docking analysis was performed using AutoDock 4.2.6 to investigate the interaction mechanism between bioflocculant-derived ligands and the target protein of *Microcystis aeruginosa* PCC7806. Docking simulations were carried out using MGLTools, employing the AutoGrid4 and AutoDock4 modules. The crystallographic three-dimensional structure of the target protein corresponding to UniProt ID Q9RNB4 was retrieved from the Protein Data Bank (PDB). Prior to docking, co-crystallized ligands and water molecules were removed. Polar hydrogen atoms were added, and Kollman charges were assigned to the receptor using AutoDock Tools. Ligand structures (Ophiocarpine, Lidocaine, Butyl isobutyl phthalate, and 1,1,3-Triethoxypropane) were obtained from PubChem and prepared by adding Gasteiger charges and defining rotatable bonds. Blind docking was performed to explore the entire protein surface for potential binding sites. The receptor was enclosed within a grid box with grid points defined along the x, y, and z axes at a grid spacing of 0.375 Å. The grid box center was set at $x = -6.516$ Å, $y = 30.278$ Å, and $z = -1.951$ Å to ensure full coverage of the protein. Docking simulations were conducted using the Lamarckian Genetic Algorithm (LGA) implemented in AutoDock4. Default parameters were applied unless otherwise specified. For each ligand, multiple docking conformations were generated, and the lowest-energy conformation predicted by the AutoDock scoring function was selected as the most favorable binding mode. Hydrogen bond interactions and amino acid contacts were analyzed to determine binding stability. The docked complexes were visualized and rendered using PyMOL (version 2.6) (Arularasu et al. 2020).

Statistical analysis

All experiments have been conducted in triplicate and the results have been represented as means ± standard deviations wherever applicable. The graph was created by Origin Pro software (2023), and a significance level of $p < 0.05$ was used.

Results and discussion

Microcystis aeruginosa cultivation

Microcystis aeruginosa was cultivated in BG-11 medium with the following parameters: pH 7, temperature of 25 °C, light intensity of 3200 lx, and a 12-h light and 12-h dark cycle (Fig. 1a). Thus, *Microcystis aeruginosa* were cultivated under the same optimum conditions in different volumes of 500 mL and 2000 mL BG-11 medium. The algal biomass development was quantified as total suspended solids (TSS) in mg/mL; the results are presented in Fig. 1b. The graph shows the increase in biomass concentration over time, measured in days. The optimum cyanobacterial cultivation required 10 to 20 days in the BG-11 medium and, for *Microcystis aeruginosa*, it took 20 days to grow and develop blooms on the water surface. Therefore, turbidity expressed in Nephelometric Turbidity Units (NTU) was also measured to assess the algal growth, illustrated in Fig. 1c. Turbidity is a measure of the cloudiness or haziness of a fluid caused by large numbers of individual particles, such as algal cells, scattering light. The average biomass concentrations of TSS in 500 mL and 2000 mL reactors were reported as 0.052 ± 0.14 day^{-1} and 0.168 ± 0.002 day^{-1}, respectively. The biomass concentration in the 2000 mL reactor was higher than that in the 500 mL reactor. The turbidity in the 500 mL reactor was 6.25 ± 0.016 NTU day^{-1}; in the 2000 mL reactor, it was 7.1 ± 0.028 NTU day^{-1}. These results obtained in this study are comparable to the findings of Bleeke et al. 2015, who cultivated three different microalgae species (*Scenedesmus acuminatus*, *Chlamydomona sreinhardtii*, and *Chlorella* sp.) and monitored their biomass concentrations of TSS and turbidity for 20 days of cultivation.

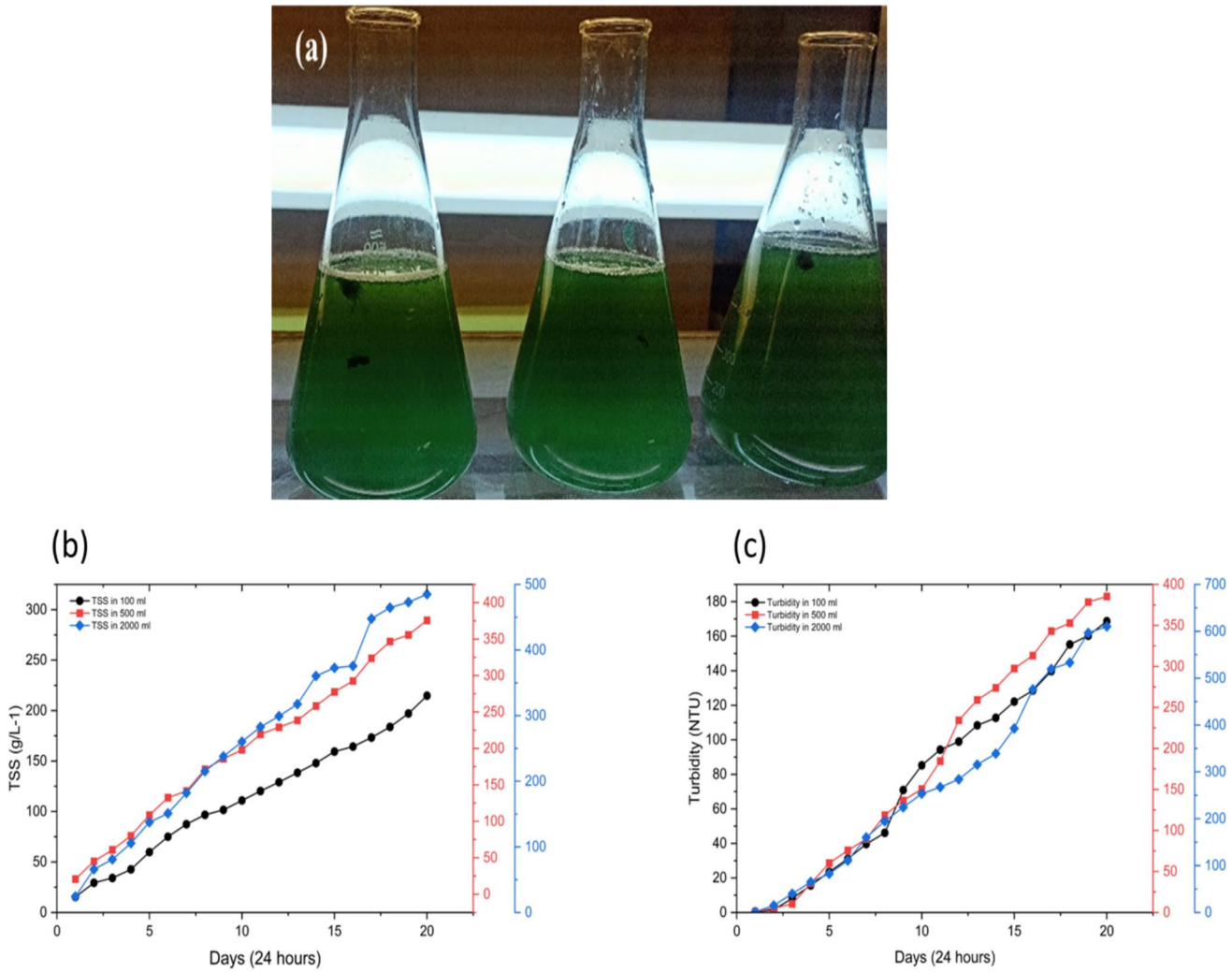

Fig. 1 Cultivation of *Microcystis aeruginosa* and biomass was evaluated each day

Fe_3O_4 synthesis and bioflocculant immobilization

The iron oxide (Fe_3O_4) nanoparticles were synthesized by using the co-precipitation method. Indeed, co-precipitation is a widely used and effective technique for producing magnetic iron oxide nanoparticles due to its advantages, including low cost, environmental friendliness, and high efficiency (Besenhard et al. 2020). Fe_3O_4 nanoparticles have been extensively studied and have garnered significant attention from researchers due to their unique properties of superparamagnetic, large surface area, and being non-toxic and biocompatible. As mentioned, the immobilization of bioflocculant on Fe_3O_4 nanoparticles can significantly reduce production costs since the immobilized bioflocculant can be reused multiple times for flocculation. This reusability is advantageous from both an economic and environmental perspective, making it a promising approach for water and wastewater treatment. Using Fe_3O_4 nanoparticles as carriers for bioflocculants offers several benefits, such as efficient separation of the flocculated particles using external magnetic fields, thus simplifying the separation and recycling processes (Qi et al. 2020a, b; Li et al. 2021). Figure 2 shows synthesis of Fe_3O_4 nanoparticles under constant stirring; the pH result is the formation of black Fe_3O_4 nanoparticles (Fig. 2a, b). The magnetic properties of the synthesized Fe_3O_4nanoparticles are demonstrated. An external magnet is shown, and the Fe_3O_4 nanoparticles are brought close to it (Fig. 2c). Finally, the Fe_3O_4 nanoparticles are dried in an oven to obtain a fine powder form (Fig. 2d). Figure 2e illustrates the process of immobilizing the bioflocculant onto the Fe_3O_4 nanoparticles. The bioflocculant solution, obtained from suitable microorganisms and purified, is added to the iron solution containing the Fe_3O_4 nanoparticles. Under suitable conditions, the bioflocculant adsorbs or chemically binds to the surface of the Fe_3O_4 nanoparticles, resulting in the immobilization of the bioflocculant. Overall, Fig. 2

Fig. 2 Synthesis and immobilization process of Fe_3O_4 nanoparticles: **a**–**b** preparation of Fe_3O_4 solution; **c**–**d** magnetic response and powder formation; **e**–**f** immobilization of bioflocculant onto Fe_3O_4 nanoparticles

depicts the step-by-step process of synthesizing Fe_3O_4 nanoparticles through co-precipitation and subsequently immobilizing a bioflocculant onto their surface. The combination of magnetic properties and immobilized bioflocculant opens up potential applications in water and wastewater treatment, offering an efficient and reusable approach for flocculation.

Characterization studies of Fe_3O_4 nanoparticle and immobilized bioflocculant

UV–visible spectroscopy

UV–visible spectroscopy was used to characterize the synthesized Fe_3O_4 nanoparticles and their functionalization with a bioflocculant. The absorption spectrum exhibited a distinct peak around 295 nm, which is characteristic of Fe_3O_4 nanoparticles. Figure 3 shows the UV–visible absorption spectra of iron oxide and bioflocculant-immobilized iron oxide nanoparticles. This observation is consistent with previous studies, where Fe3O4 nanoparticles typically show absorption in the range of 290–310 nm due to their electronic transitions (Karpagavinayagam and Vedhi 2019; Justin et al. 2017).

Upon immobilization of the bioflocculant onto the Fe_3O_4 nanoparticles, additional absorption peaks were observed at approximately 250 nm and 280 nm. These wavelengths are commonly associated with aromatic compounds like aromatic amino acids (e.g., tryptophan, tyrosine, and phenylalanine) and nucleic acids. They can also serve as indirect indicators of proteinaceous materials. Proteins containing aromatic residues absorb strongly at these wavelengths due to π-π* transitions within the aromatic rings. Although polysaccharides themselves do not typically absorb in this region, bioflocculants often consist of complex biomolecular assemblies, including glycoproteins or protein–polysaccharide conjugates, in which aromatic amino acid residues contribute to UV absorption.

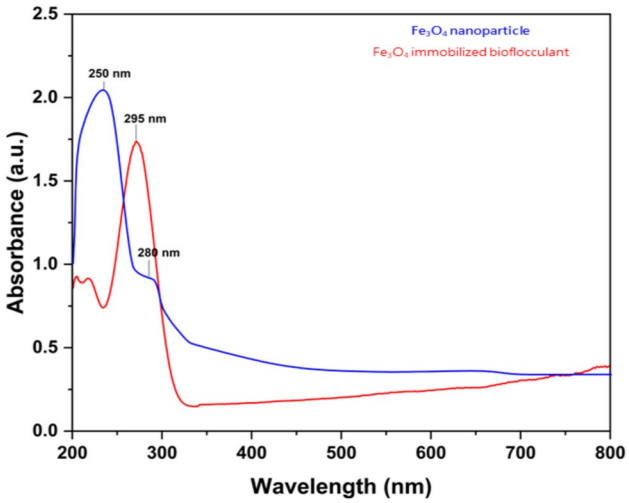

Fig. 3 UV–Vis spectrum of Fe_3O_4–bioflocculant composite showing characteristic absorption peaks associated with proteinaceous functional groups

Therefore, the presence of peaks at 250 nm and 280 nm suggests the existence of aromatic moieties, likely originating from protein components of the bioflocculant. This provides evidence supporting the successful immobilization of the bioflocculant onto the Fe_3O_4 nanoparticles (Maliehe et al. 2016). Thus, the UV–visible analysis confirms both the synthesis of Fe_3O_4 nanoparticles and the attachment of the bioflocculant.

Fourier-transform infrared spectroscopy (FTIR)

Bioflocculant's successful immobilization onto the Fe3O4 nanoparticles is provided in Fig. 4 The analysis of the functional groups observed in the infrared spectrum (IR) helps identify the chemical bonds in the immobilized bioflocculant and the Fe_3O_4 nanoparticles. The peaks from the IR spectrum were observed at 3360 cm^{-1}, 2982.81 cm^{-1}, and 2881.65 cm^{-1}, which are characteristic of O–H stretching. These peaks are commonly associated with hydroxyl and carboxyl groups (Manivasagan et al. 2015). A strong peak at 1544.98 cm^{-1} indicates the presence of a nitro compound with N–O stretching. This observation suggests the involvement of nitrogen-containing groups in the immobilization process. The peak at 1136.07 cm^{-1} was attributed to the C-O bond, indicating the presence of sugars in the immobilized bioflocculant and polysaccharide sugars are a common component in bioflocculant (Xia et al. 2022). The peak observed at 1072.42 cm^{-1} corresponds to the O–H bond of a carboxylic acid. This peak further confirms the presence of carboxyl groups in the immobilized bioflocculant. A small absorption peak at 563.21 cm^{-1} and 472.56 cm^{-1} represents the presence of the alkyl halide group. These functional groups suggest the involvement of alkyl halides, organic compounds, in the immobilization process (Xia et al. 2022). The strong stretching absorption bands observed at 583.56 cm^{-1} and 563.21 cm^{-1} are characteristic of Fe_3O_4 nanoparticles. These peaks confirm the presence of magnetite (Fe_3O_4) in the bare Fe_3O_4 nanoparticles and the bioflocculant-immobilized nanoparticle spectra. The intense peaks from 1100 to 1200 cm^{-1} are attributed to the C-O group bend. This observation indicates that the immobilized bioflocculant successfully interacts with the Fe_3O_4 nanoparticles, as these bands were related to the bonding between the bioflocculant and the Fe_3O_4 nanoparticles (Lucane et al. 2022).

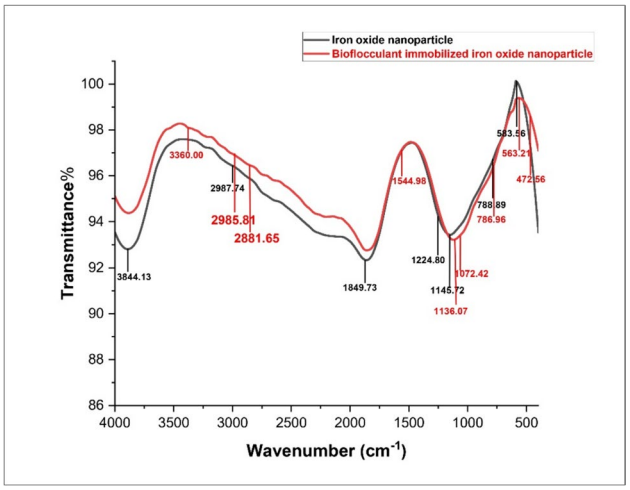

Fig. 4 Infrared spectrum of bioflocculant and bioflocculant-immobilized iron oxide nanoparticles

Scanning electron microscopy (SEM) analysis

The morphological characterization of Fe_3O_4 nanoparticles and bioflocculant-immobilized Fe_3O_4 nanoparticles as seen by scanning electron microscopy (SEM) is shown in Fig. 5. The SEM image shown in Fig. 5a shows that the free Fe_3O_4 nanoparticles have a spherical shape. The spherical morphology is a common characteristic of many nanoscale materials, including Fe_3O_4 nanoparticles. Figure 5b presents the SEM image of the bioflocculant-immobilized Fe_3O_4 nanoparticles. The image shows that the immobilized nanoparticles also exhibit a spherical shape, similar to the free nanoparticles. However, the bioflocculant coating on the surface of the nanoparticles may lead to changes in the size and overall structure compared to the free nanoparticles. The size of the free Fe_3O_4 nanoparticles was measured in the range of 50 to 70 nm, while the size of the bioflocculant-immobilized Fe_3O_4 nanoparticles was measured to be slightly larger, in the range of 70 to 80 nm. The observed

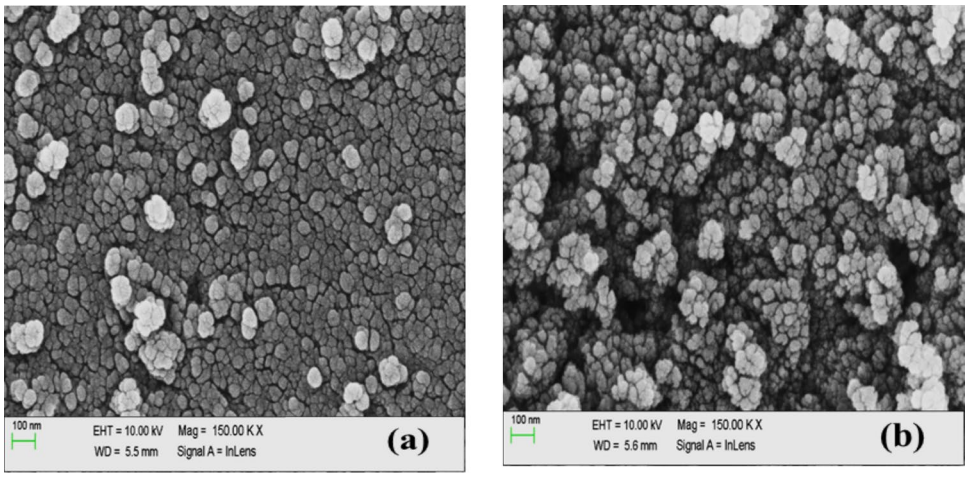

Fig. 5 Morphology of the Fe3O4 nanoparticles (**a**) and bioflocculant-immobilized Fe3O4 nanoparticles (**b**) was analyzed by scanning electron microscope

morphology distribution and size range of the iron oxide nanoparticles in this study align with the findings of previous research conducted by Prodan et al. 2013. These results suggest that the synthesis and immobilization methods used in the current study are consistent with earlier investigations, and the results were similar to the existing literature.

Energy-dispersive X-ray analysis (EDX)

The elemental composition of the synthesized materials was analyzed using Energy-Dispersive X-ray spectroscopy (EDX), and the quantitative data are summarized in Table 1. The pristine iron oxide nanoparticles predominantly consist of iron (Fe – 76.35 wt%) and oxygen (O – 23.65 wt%), consistent with the expected stoichiometry of magnetite (Fe_3O_4). Following immobilization with the bioflocculant, a substantial reduction in iron content (22.15 wt%) and a marked increase in oxygen content (55.69 wt%) were observed. Additionally, new elemental signals corresponding to carbon (C – 18.41 wt%), nitrogen (N – 1.05 wt%), sulfur (S – 0.5 wt%), and phosphorus (P – 1.2 wt%) appeared in the spectrum. The emergence of C and N confirms the presence of proteinaceous and polysaccharide components of the microbial-derived bioflocculant on the nanoparticle surface. The detection of sulfur may be attributed to sulfur-containing amino acids (e.g., cysteine or methionine) present in the bioflocculant structure. The presence of phosphorus is attributed to phosphate functional groups naturally occurring in extracellular polymeric substances (EPS) produced by the bioflocculant-producing microorganism. Phosphate groups contribute to structural stability and functional activity in flocculation mechanisms. In addition, residual phosphate from culture medium components (e.g., KH_2PO_4 or NaH_2PO_4) may remain associated with the purified bioflocculant. Similar observations of phosphorus incorporation in Fe_3O_4-immobilized bioflocculants have been reported by Dlamini et al. (2020) and Selepe et al. (2022). Overall, the EDX results provide strong evidence for the successful immobilization of the bioflocculant onto Fe_3O_4 nanoparticles, supporting the compositional data presented in Table 1.

Table 1 Elemental analysis of the Fe_3O_4 and bioflocculant-immobilized Fe_3O_4 nanoparticle

Elements	Samples	
	Iron oxide nanoparticle (wt%)	Bioflocculant-immobilized iron oxide nanoparticle (wt%)
O K	23.65	55.69
Fe K	76.35	22.15
C	-	18.41
N	-	1.05
S	-	0.5
P	-	1.2

Dynamic Light Scattering (DLS)

The Dynamic Light Scattering (DLS) technique is used to determine the size distribution of particles in a colloidal or nanoparticle suspension. It has commonly been applied to study particles ranging from molecules and nanoparticles to larger macromolecules and aggregates. In Fig. 6, the size distribution and intensity of the Fe_3O_4 nanoparticles were investigated using Dynamic Light Scattering (DLS) with a Zetasizer instrument (Zetasizer-M3-PALS, Malvern Panalytical). The data presented in the figure indicates that the hydrodynamic size distribution of the Fe_3O_4 nanoparticles was arranged at approximately 80 d.nm. Comparing the results from previous studies, Abbasi et al. 2020 reported a Fe_3O_4 nanoparticle size of 293.4 d·nm, while Vélez et al. (2016) reported a size of 99.56 d·nm.

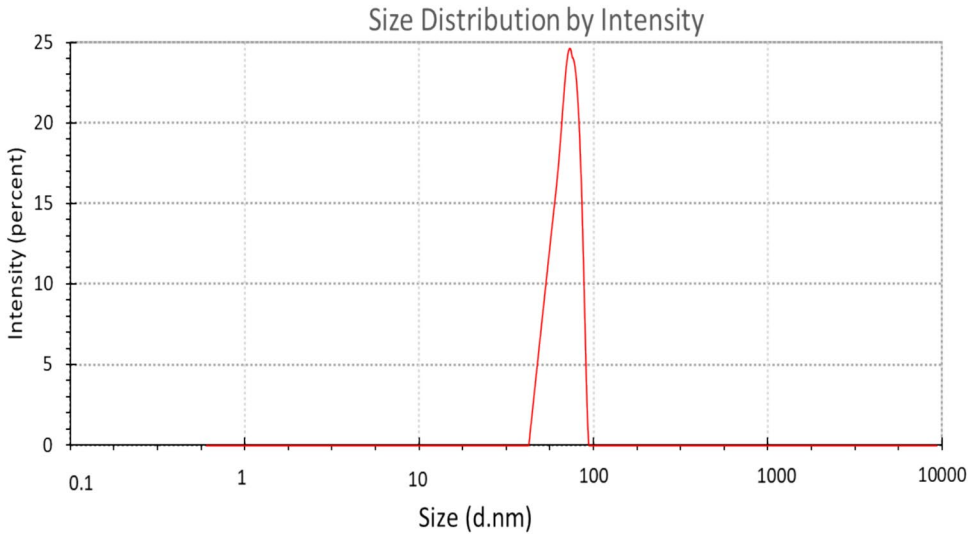

Fig. 6 Size distribution analysis of the bioflocculant-immobilized Fe3O4 nanoparticles

High-resolution transmission electron microscopy (HR-TEM)

The synthesized and bioflocculant-immobilized Fe_3O_4 nanoparticle morphology was analyzed through a transmission electron microscope (TEM). Therefore, free Fe_3O_4 and bioflocculant-immobilized Fe_3O_4 nanoparticles were depicted in Fig. 7a, b. Correspondingly, both free and immobilized nanoparticle shapes would appear spherical. Then, the TEM images exhibit the bioflocculant coated around the Fe_3O_4 nanoparticles, confirming that the bioflocculant was successfully immobilized with Fe_3O_4 nanoparticles. Figure 7c shows the measurement of the particle size of the Fe_3O_4 nanoparticles. Therefore, the average size of the nanoparticles was measured and observed as 12-nm size. This size distribution indicates that the nanoparticles were relatively uniform in size and maintained their spherical shape. In Fig. 7d, the particle size of the bioflocculant-immobilized Fe_3O_4 nanoparticles was measured, and the average size of the immobilized nanoparticles was 18 nm. Therefore, increases in particle size after immobilization were expected, as the bioflocculant coating adds a layer to the nanoparticles. Similar outcomes were noted by Stolyar et al. (2021), who also reported that the synthesized polysaccharide was successfully coated with iron oxide nanoparticles and observed in characterization studies.

X-ray diffraction analysis (XRD)

Figure 8 shows the X-ray diffraction (XRD) diffractograms of both the Fe_3O_4 nanoparticles and the bioflocculant-immobilized Fe_3O_4 nanoparticles for the analysis of their crystallographic structures and characteristic peaks. The XRD diffractogram of Fe_3O_4 nanoparticles shows characteristic peaks at 2θ values of 25.9°, 33.2°, 37.3°, 38.9°, 47.6°, and 52.0°. Corresponding Miller indices peaks correspond to the (220), (311), (400), (422), (511), and (440) crystallographic planes of the Fe_3O_4 nanoparticles. Similarly, the bioflocculant-immobilized Fe_3O_4 nanoparticles diffractogram displays characteristic peaks at 2θ values of 30.2°, 35.5°, 43.2°, 57.2°, 62.8°, and 90.1°. These peaks correspond to the crystallographic planes of the Fe_3O_4 nanoparticle and bioflocculant-immobilized Fe_3O_4 nanoparticles. Therefore, XRD diffractogram peaks observed in the current study for both the Fe_3O_4 nanoparticles and the bioflocculant-immobilized Fe_3O_4 nanoparticles are consistent with the findings of previous research conducted by Fraga-Garcia et al. (2018) and Zhao et al. (2015). These studies also reported similar XRD peak positions and Miller indices for Fe_3O_4 nanoparticles. The presence of characteristic peaks corresponding to specific crystallographic planes confirms the formation of magnetite in the Fe_3O_4 nanoparticles. Additionally, the observed XRD peaks for the bioflocculant-immobilized Fe_3O_4 nanoparticles suggest that the immobilization process does not significantly alter the crystal structure of the nanoparticles.

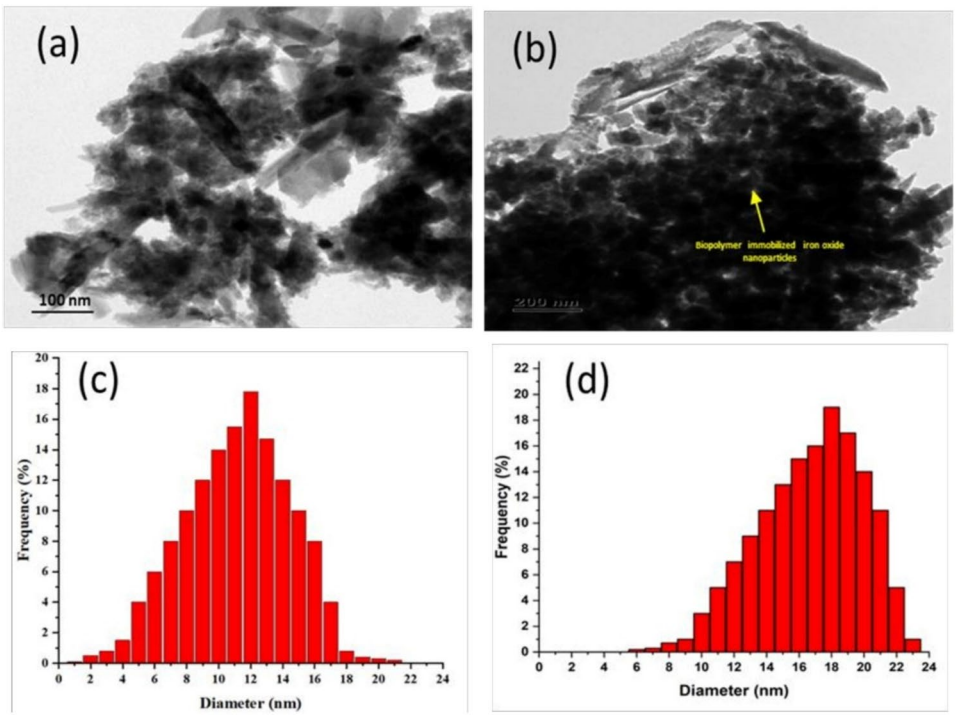

Fig. 7 High-resolution transmission electron microscopy (HR-TEM) image showing uniform distribution of the Fe3O4 nanoparticles (**a**), bioflocculant-immobilized Fe3O4 nanoparticles (**b**), size distribution of the free Fe3O4 nanoparticle (**c**), and bioflocculant-immobilized Fe3O4 nanoparticles (**d**). Free Fe3O4 nanoparticle

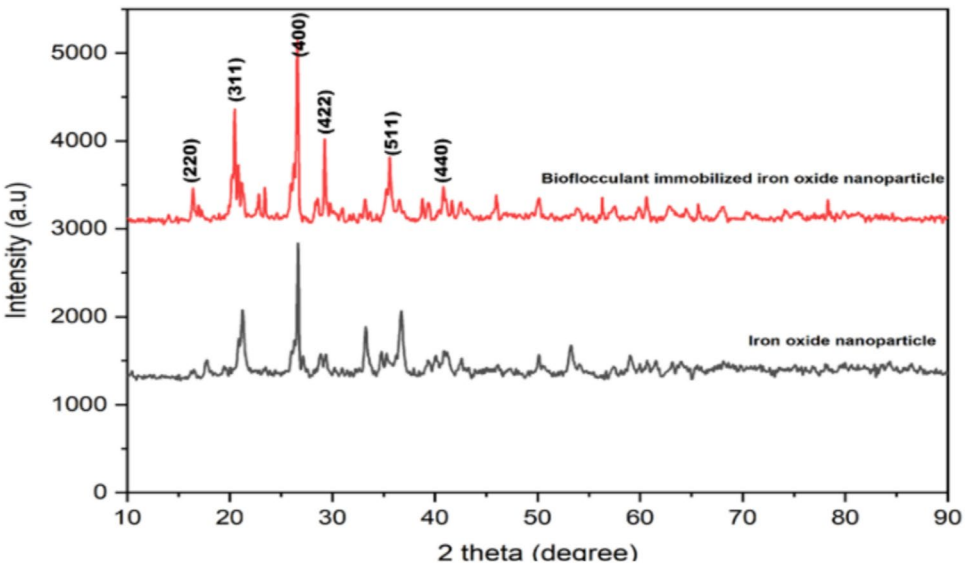

Fig. 8 X-ray diffraction (XRD) pattern of the Fe3O4 nanoparticle and bioflocculant immobilized Fe3O4 nanoparticles

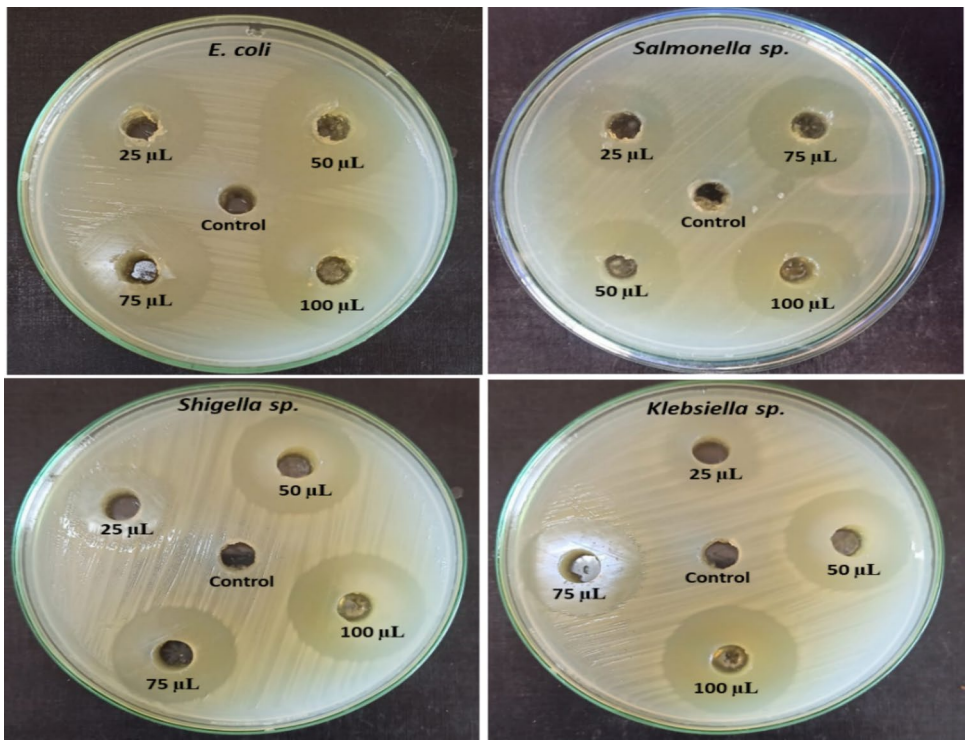

Fig. 9 Antibacterial activity properties of bioflocculant-immobilized Fe3O4 nanoparticles against water pathogens

Antibacterial activity

In this study, the antibacterial potential of the bioflocculant-immobilized Fe_3O_4 nanoparticles was tested against common water pathogens, such as *E. coli*, *Klebsiella* sp., *Salmonella* sp., and *Shigella* sp., as shown in Fig. 9. The antibacterial activity of bioflocculant-immobilized Fe_3O_4 nanoparticles against all four pathogens was evaluated. The bioflocculant-immobilized Fe_3O_4 nanoparticles showed remarkable properties against all four bacterial strains, as revealed by well diffusion and the loading sample values ranging from 25 to 100 µL (Table 2). Our study found that *E. coli*, *Klebsiella*, *Salmonella*, and *Shigella* were significantly inhibited by the immobilized bioflocculant in different concentrations of 25 µL, 50 µL, 75 µL, and 100 µL, respectively. Based on the results observed, bioflocculant-immobilized Fe_3O_4 nanoparticles exhibited prominent antibacterial activity against all test pathogens. Therefore, Fe_3O_4 immobilized bioflocculant served as a good natural disinfectant in treating wastewater. Similarly, Jeong et al. (2017) specifically reported that

Table 2 Antibacterial activity of bioflocculant-immobilized Fe_3O_4 nanoparticles' zone of inhibition against water pathogenic microorganisms

Name of the test organism	Zone of inhibition (mm)				
	25 µL	50 µL	75 µL	100 µL	Positive control
E. coli	12	14	15	16.5	10
Salmonella	13	13	14	17	10
Shigella	11.5	13	14.5	16	10.5
Klebsiella	10	11	13	15.5	11

extracellular polymeric substances (EPS) produced by *Lactobacillus kefiranofaciens* DN1 exhibited inhibitory effects against various food-borne bacterial pathogens.

Effect of Fe_3O_4 nanoparticle immobilized bioflocculant on Microcystis aeruginosa removal

Effect of dosage concentration on flocculation of Microcystis aeruginosa

It is essential to determine the optimal dosage concentration of bioflocculant to reduce the cost and appropriate flocculation of *Microcystis aeruginosa*. The optimum dosage concentration of bioflocculant immobilized iron oxide nanoparticles was found to be 20 mg/mL (Fig. 10), which exhibited maximum flocculating activity of 95.65%. Further, insufficient dosage concentration can reduce the flocculation efficiency of bioflocculant and bioflocculant immobilized iron oxide nanoparticles. Similar results were reported by Zou et al. (2018), and Govarthanan et al. (2020), which were well in accordance with our study.

Effect of pH

The effect of pH on the flocculation efficiency of bioflocculant immobilized iron oxide nanoparticles was determined to analyze their sensitivity towards various pH. The optimum pH for maximum flocculation of *Microcystis aeruginosa* by bioflocculant immobilized iron oxide nanoparticles observed to be 8 (Fig. 11), which exhibited maximum flocculating activity of 96.83%, respectively. Further, the flocculation potential of bioflocculant immobilized iron oxide nanoparticles was lowered when pH was changed to extreme alkaline or acidic conditions. This could be attributed to the fact that extreme alkaline or acidic conditions could disrupt or denature. The flocculation efficiency failed to remove algal blooms. However, bioflocculant immobilized iron oxide nanoparticles retain their flocculation efficiency of 90% in extreme alkaline and acidic conditions, which indicates that they are insensitive to a wide range of pH (3 to 12).

Effect of temperature

The effect of temperature on the flocculation efficiency of bioflocculant immobilized iron oxide nanoparticles were determined to identify their temperature sensitivity property. The optimum temperature for maximum flocculation of *Microcystis aeruginosa* by bioflocculant immobilized iron oxide nanoparticles was 30 °C. The maximum flocculation efficiency of 95.26% was achieved by bioflocculant

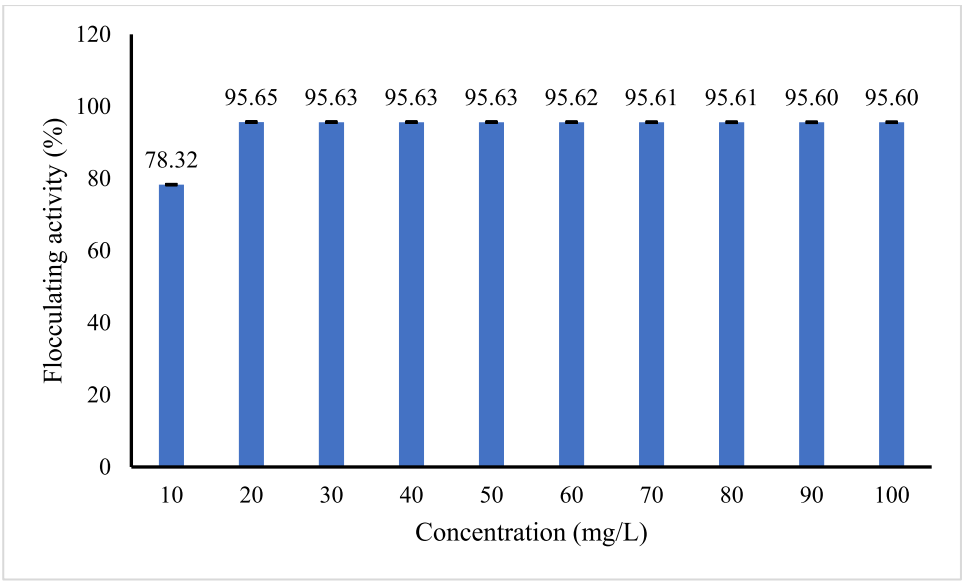

Data are expressed as Mean±SD (n=3)

Fig. 10 Effect of Dosage concentration of the immobilized bioflocculant on *Microcystis aeruginosa* removal

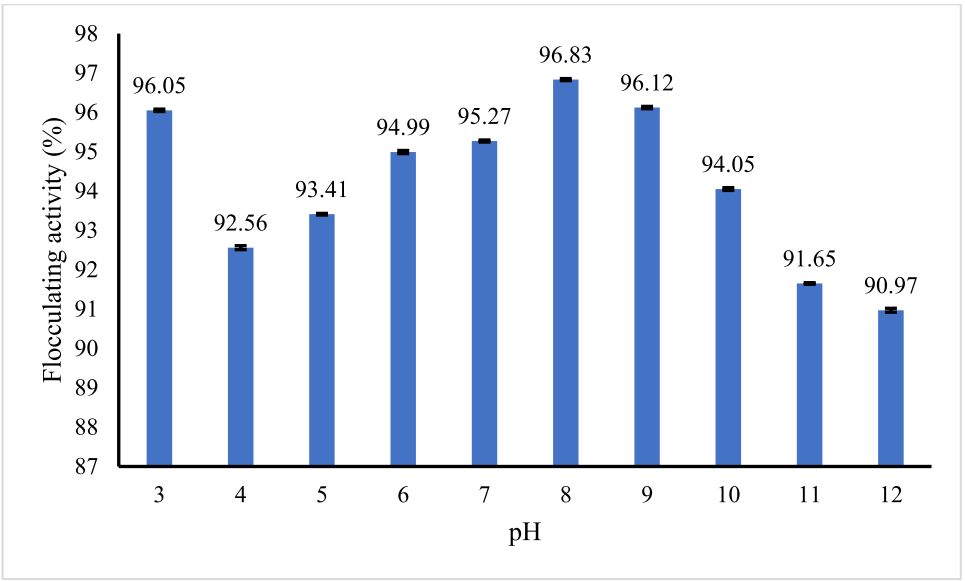

Fig. 11 Effect of pH in the *Microcystis aeruginosa* removal by the immobilized biofloculant

Data are expressed as Mean±SD (n=3)

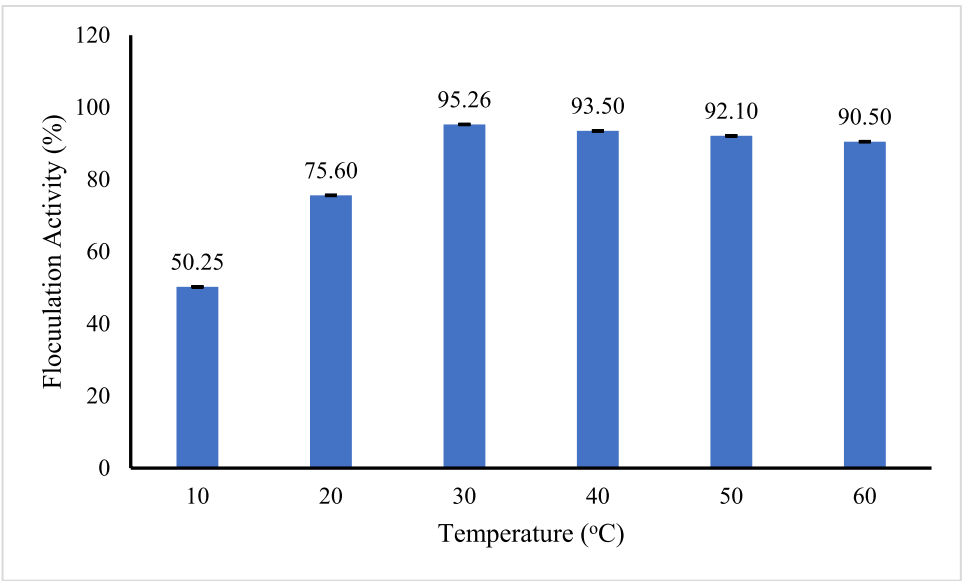

Fig. 12 Effect of different temperatures in Microcystis aeruginosa removal by the immobilized bioflocculant

Data are expressed as Mean±SD (n=3)

immobilized iron oxide nanoparticles (Fig. 12). Further, an increase or decrease beyond the optimum temperature would reduce the flocculation efficiency of free bioflocculant and bioflocculant immobilized iron oxide nanoparticles. This could be attributed to the fact that increased temperature may denature the proteins, reduce the flocculation potential, and decrease the temperature, causing floc formation that would reduce the flocculation process. Our results were in well accordance with the earlier study by Zhang et al. (2019).

Effect of stirring speed

The optimum stirring speed for maximum flocculation of *Microcystis aeruginosa* by bioflocculant immobilized iron oxide nanoparticles was 120 rpm. The maximum

flocculation efficiency of 96.86% was achieved by bioflocculant immobilized iron oxide nanoparticles, respectively (Fig. 13). Further, an increase or decrease beyond the optimum stirring speed, the flocculation efficiency was lowered. This could be attributed to the fact that high-speed stirring may break the flocs and disperse the cells back to the water, whereas low-speed stirring may fail to disperse the flocculant uniformly in the water.

Effect of stirring time

The stirring time plays a vital role in floc formation, where algal cells get adsorbed to bioflocculant through bridging or charge neutralization during the stirring period. The effect of stirring time on the flocculation of *Microcystis aeruginosa* by bioflocculant immobilized iron oxide nanoparticles was observed to be 120 rpm for 5 min. The maximum 96.06% flocculation efficiency were observed for bioflocculant immobilized iron oxide nanoparticles (Fig. 14). Further, an increased stirring time causes lower flocculation efficiency of free bioflocculant and bioflocculant immobilized iron oxide nanoparticles, which is due to the breakage of the flocculant chain and limiting the size of floc's formation.

Effect of settling time

The settling time is essential in achieving maximum flocculation of Microcystis aeruginosa by bioflocculants. The effect of settling time on the flocculation of Microcystis aeruginosa by bioflocculant immobilized iron oxide nanoparticles was observed to be 60 min. The maximum flocculation efficiency of 97.05% was observed for bioflocculant immobilized iron oxide nanoparticles, respectively (Fig. 15). Further, the flocculation potential was drastically increased for every 10 min of time interval. This indicated that settling time may aid floc formation and attain maximum flocculation efficiency of bioflocculant immobilized iron oxide nanoparticles.

Reusaility of bioflocculant-immobilized Fe_3O_4 nanoparticles

For *Microcystis aeruginosa* removal, bioflocculant-immobilized Fe_3O_4 nanoparticles were applied under optimized conditions: 30 mg/L dosage, pH 6.5, temperature 37 °C, stirring speed 120 rpm, and 60 min settling time. Figure 16a illustrates the flocculation process, where the algal cells were removed using an external magnet after treatment. The formed flocs were filtered, and the pH was adjusted to between 10 and 12 using 1 N NaOH or HCl to separate algal cells from the immobilized bioflocculant (Wang et al. 2018; Seo et al. 2014). The morphology of the filtered flocs was observed under SEM, as shown in Fig. 16c confirming effective flocculation.

The reused bioflocculant was recollected using external magnets and applied repeatedly until the flocculation efficiency dropped to zero. Figure 16b shows that flocculating activity remained above 90% during the first to fourth reuse cycles. However, a noticeable decline was observed from the fifth reuse onward, with efficiency dropping from 71.38% to 8.18% by the ninth cycle. This reduction may be attributed to the loss of electrostatic interaction due to gradual leaching or degradation of the polymeric bioflocculant, which

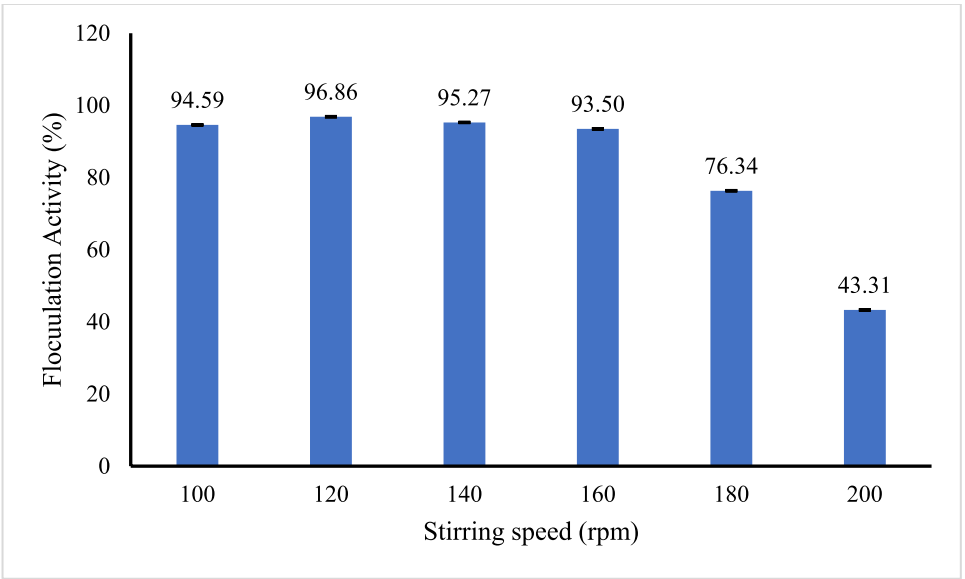

Data are expressed as Mean±SD (n=3)

Fig. 13 Effect of stirring speed for the bioflocculant-immobilized Fe3O4nanoparticles in*Microcystis aeruginosa* removal

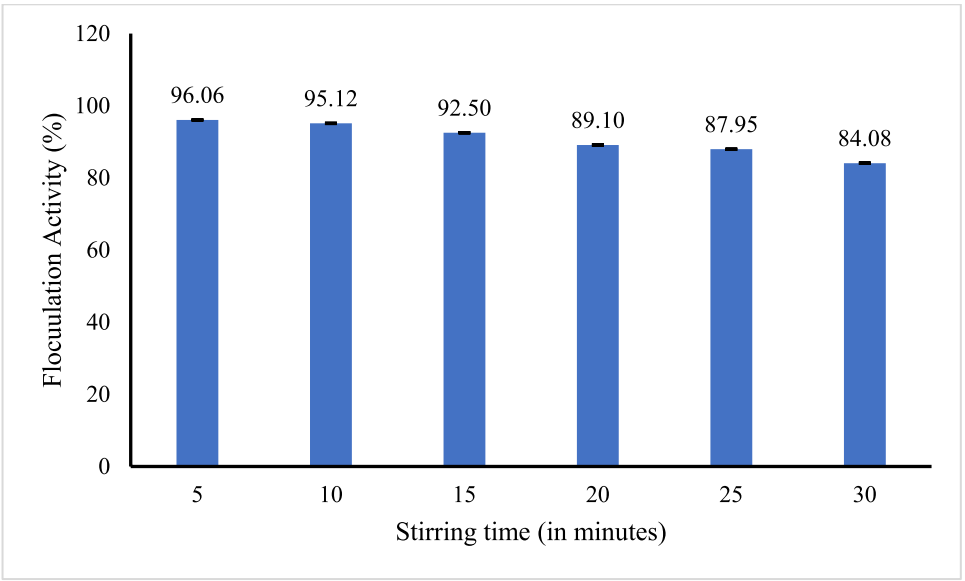

Fig. 14 Effect of stirring time for the bioflocculant-immobilized Fe3O4 nanoparticles in*Microcystis aeruginosa* removal

Data are expressed as Mean±SD (n=3)

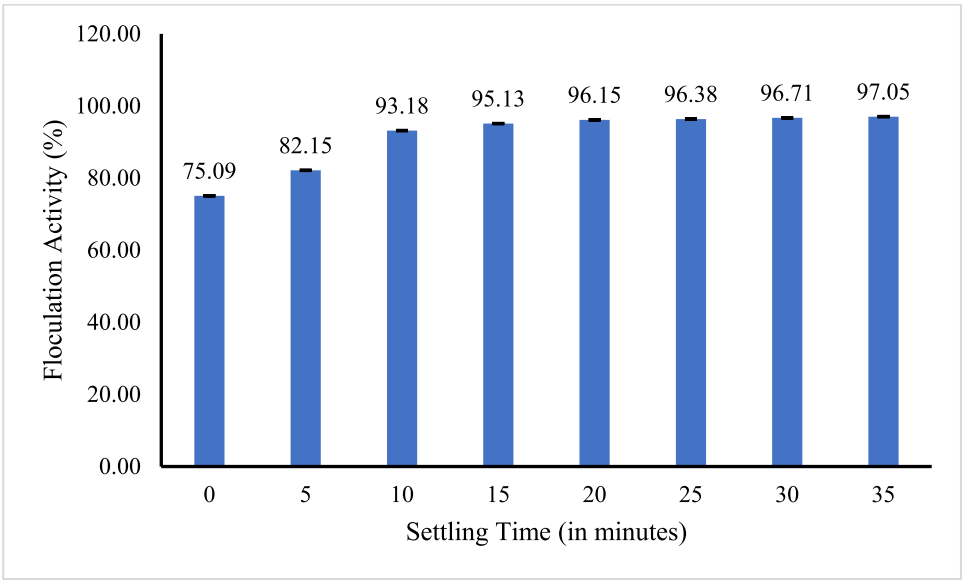

Fig. 15 Effect of settling time for the bioflocculant-immobilized Fe3O4nanoparticles in*Microcystis aeruginosa* removal

Data are expressed as Mean±SD (n=3)

weakens its binding ability. Although the current study did not include FTIR or SEM analysis after each reuse cycle, these results suggest that bioflocculant detachment or degradation plays a role in reducing performance.

Despite this, the Fe_3O_4nanoparticles retained their magnetic responsiveness throughout the cycles, aiding in efficient separation and recovery. Overall, the system demonstrated cost-effectiveness, allowing for at least four reuse cycles, thereby reducing the bioflocculant production cost. This is in line with earlier reports, such as Markeb et al. (2019) where Fe_3O_4–chitosan composites were successfully reused six times for harvesting *Scenedesmus* sp. microalgae. Future work will include post-reuse structural and functional analysis to better understand the mechanisms behind performance decline and to further improve reusability.

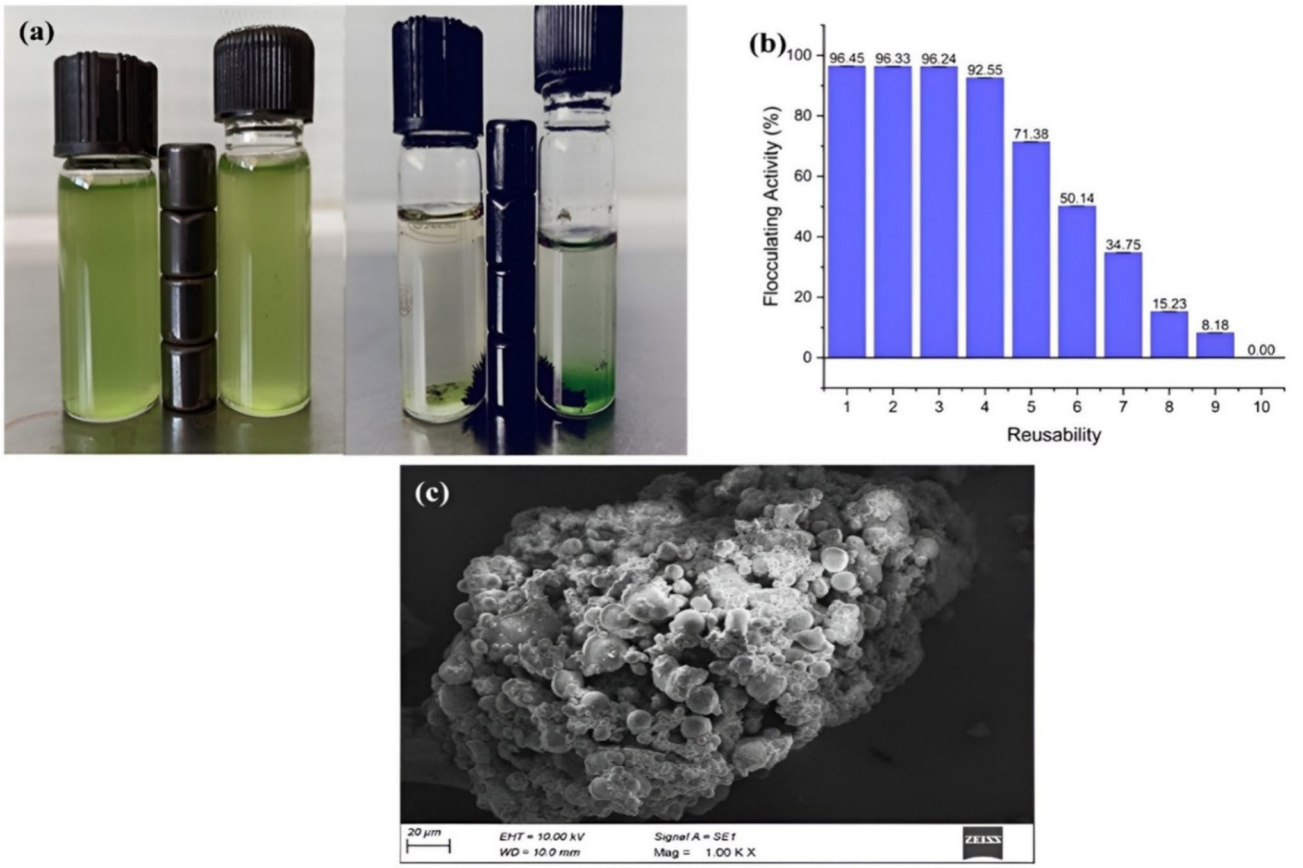

Fig. 16 Microcystis aeruginosa removal and reusability with bioflocculant-immobilized Fe3O4 nanoparticles flocculation activity. **a** Recovery after treatment using magnet. **b** Reusability percentage, **c** Microscopic observation of adsorbed algae in bioflocculant

Flocculation mechanism

The flocculation mechanism could be explained through zeta potential parameters, which measure the surface charge of the microalgae. The average zeta potential of the bioflocculant, Fe_3O_4 nanoparticles, and bioflocculant-immobilized NPs have -29.48 ± 1.5 mV, -31.4 ± 2.2 mV, and -34.15 ± 3.1 mV, respectively. Similarly, the zeta potential on microalgae before treatment was also negative (-10.6 mV) at pH 6.5. In addition, the zeta potential of *Microcystis aeruginosa* microalgae after treatment with bioflocculant was observed to be -47.3 ± 6.13 mV. Moreover, greater zeta potential is more stable in the flocculation to floc the algal cells (Bisht and Lal 2019). From this study, the results through zeta potential analysis suggest that the most probable mechanism, which could define a bridging mechanism, involves the flocculation process. Figure 17 schematic illustration represents the possible mechanism of the bridging mechanism taking place to flocculate the *Microcystis aeruginosa* and the bioflocculantFe_3O_4 nanoparticles were recollected by external magnet to reuse multiple times. Bridging mechanism involves formation of a three-dimensional complex structure in which the polysaccharide bioflocculant acts as a bridging element between the bioflocculant and *Microcystis aeruginosa*. This can be ascribed to the presence of hydroxyl groups in the bioflocculant, as analyzed by FTIR. In the presence of hydroxyl groups in bioflocculant, (i) interaction between bioflocculant and *Microcystis aeruginosa* cells occurs due to ionic bonding and (ii) H-bonding aids bioflocculant in being adsorbed onto the surface of *Microcystis aeruginosa* cells. In addition, a polysaccharide backbone with active sites may also be considered as one of the factors for the high flocculation activity of bioflocculant. Correspondingly, bioflocculant-immobilized with Fe_3O_4 nanoparticles provide stability and thermal stability, possess a high surface area, and are recollected by external magnets, easing the flocculation process to nearly cut down the production cost. Bridging mechanisms have also been proposed earlier for bioflocculation from *Serratia marcescens*, *Bacillus megaterium* strain PL8, and *Bacillus subtilis* ZHX3 bioflocculant by Kurniawan et al. (2022); Pu et al. (2020) and Xia et al. (2022).

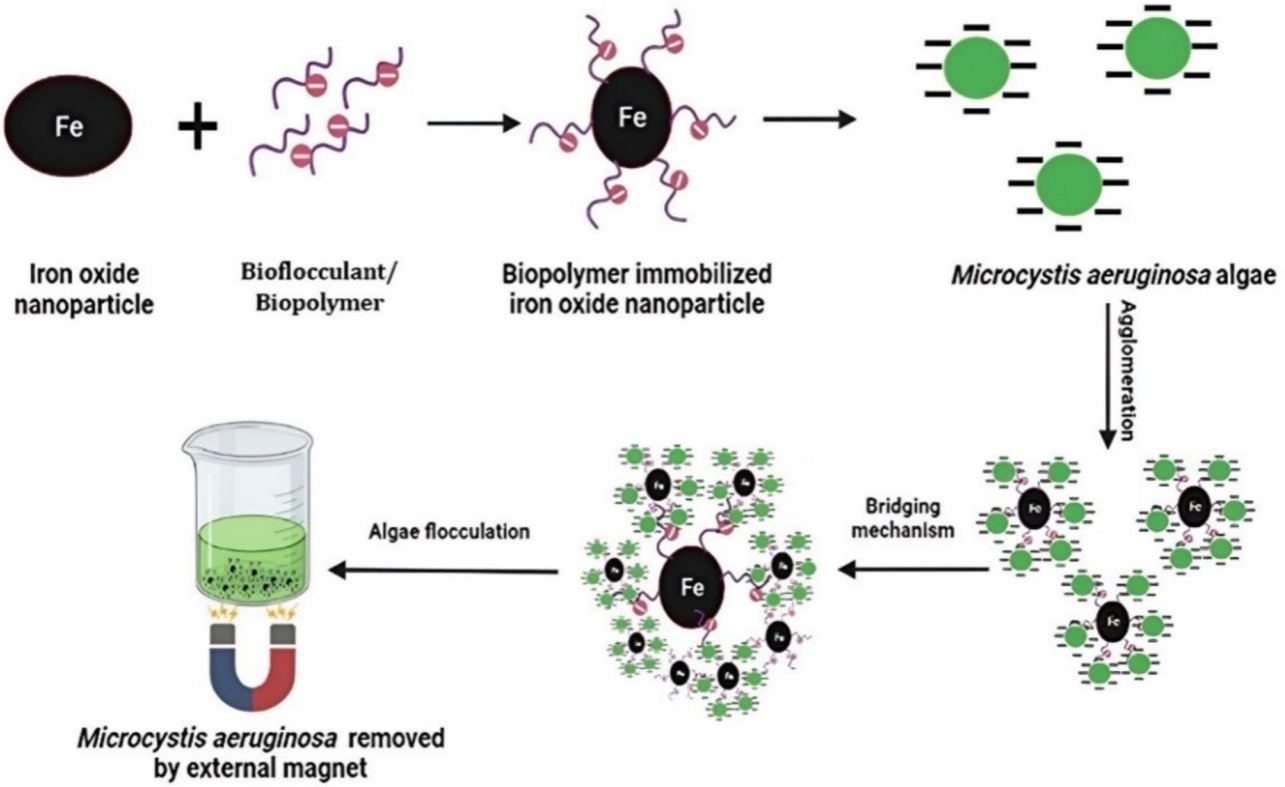

Fig. 17 Schematic representation of the possible mechanism of *Microcystis aeruginosa* flocculation by immobilized bioflocculant

Physicochemical properties of harmful algal water before and after treatment

Under certain environmental conditions, harmful algal blooms (HABs) may occur, resulting in excessive accumulation of algal biomass, reduced dissolved oxygen, and the possible production of toxins. The health of humans can be adversely affected by an array of algae species that can produce hazardous substances in the water. For the water treatment process, flocculation is usually applied to remove the algal cells from the water through a downstream method (Ren et al. 2022). The physicochemical characteristics of *Microcystis aeruginosa*-polluted water before and after treatment with Fe_3O_4-immobilized bioflocculant are summarized in Table 3. Prior to treatment, the algal water exhibited elevated levels of turbidity (185.4 NTU), TSS (164 mg/L), TDS (4200 mg/L), BOD (64 mg/L), COD (362 mg/L), total hardness (650 mg/L), chloride (2812 mg/L), nitrate nitrogen (200 mg/L), fluoride (4.427 mg/L), and dissolved phosphate (5.94 mg/L), indicating severe deterioration in water quality due to harmful algal bloom conditions. Upon treatment, substantial reductions were observed: turbidity decreased to 4.1 NTU, TSS to 78.5 mg/L, TDS to 159.14 mg/L, BOD to 3.0 mg/L, COD to 18.0 mg/L, total hardness to 184 mg/L, chloride to 214 mg/L, nitrate nitrogen to 42 mg/L, fluoride to 0.174 mg/L, and dissolved phosphate to 1.17 mg/L. The pH was adjusted from alkaline (9.11) to near neutral (7.25). Microbial indicators such as fecal coliform and *E. coli* were absent both before and after treatment. The flocculating activity was recorded at 96.55%, confirming high removal efficiency. The treated water parameters were found to be within the permissible limits specified by the Bureau of Indian Standards under IS 10500. However, although physicochemical and microbial parameters met drinking water standards, residual microcystins and cytotoxicity were not assessed in the present study. Therefore, further toxicological evaluation is recommended before confirming suitability for potable use.

Comparison of performance of bioflocculant, bioflocculant-immobilized Fe_3O_4 nanoparticles, and traditional flocculants

The comparative analysis of the flocculation efficiency of different flocculants against *Microcystis aeruginosa* is crucial for understanding the performance of the Fe_3O_4 immobilized bioflocculant in removing harmful algae from water sources. The flocculation activities of different flocculants, such as the Fe3O4 immobilized bioflocculant and traditional synthetic flocculants, are clearly compared in Table 4 at an equivalent dosage of 20 mg/L. This standardized dosage was

Table 3 Physicochemical parameters of the harmful algal polluted water before and after being treated with Fe_3O_4 immobilized bioflocculant

Characteristics	Unit	Before	After Fe_3O_4
Color	Hazen	50	< 5.0
Odor	-	Objectionable	Agreeable
TSS	mg/L	164	78.5
TDS	mg/L	4200	159.14
pH@25 °C		9.11	7.25
Temperature		27.2	27.5
Turbidity	NTU	185.4	4.1
BOD	mg/L	64	3.0
COD	mg/L	362	18.0
Total alkalinity $CaCo_3$	mg/L	160	52
Total hardness as $CaCo_3$	mg/L	650	184
Calcium (ca)	mg/L	320	70
Magnesium	mg/L	180	26
Residual sodium carbonate	mg/L	3.16	1.26
Chloride	mg/L	2812	214
Residual free chlorine	mg/L	124	0.25
Nitrate nitrogen	mg/L	200	42
Fluoride	mg/L	4.427	0.174
Fecal coliform	MPN/100 mL	0	0
E. coli	Presence/absence	0	0
Dissolved phosphate	mg/L	5.94	1.17
Sulfate	mg/L	94	41
Sulfide	mg/L	18.4	9.2

selected to ensure a fair and direct comparison of flocculation performance.

The commercially available flocculants, such as ferric chloride, alum, polyethyleneimine, and polyacrylamide, achieved flocculation efficiencies of 85.42%, 95.12%, 82.10%, and 92.5%, respectively. These values varied slightly based on the intrinsic properties of each flocculant but were all measured under identical treatment conditions and concentrations. Under the same optimized conditions and dosage, the Fe_3O_4 immobilized bioflocculant demonstrated a maximum flocculation efficiency of 96.4% against *Microcystis aeruginosa*, indicating superior performance.

This result suggests that the Fe_3O_4 immobilized bioflocculant is highly effective in removing harmful algae and performs better than the tested synthetic flocculants at an equivalent dosage. The use of a standardized concentration strengthens the validity of this comparison. Therefore, the Fe_3O_4 immobilized bioflocculant shows great potential as an efficient and environmentally friendly alternative for harmful algal removal. Overall, the findings demonstrate its suitability for sustainable water treatment and environmental remediation applications. In addition, this study suggests that magnetic nanoparticles with bioflocculant immobilization offer rapid methods to remove harmful algal blooms. Therefore, Fe_3O_4–bioflocculant should be explored and developed in future harmful algal bloom removal studies (Lucena et al. 2022; Li et al. 2020).

In silico studies of the molecular docking

Molecular docking was performed to elucidate the possible interaction mechanism between bioflocculant-derived compounds and the target protein of *Microcystis aeruginosa* PCC7806. The ligand molecules were previously identified through GC–MS analysis (Jayaprakash et al. 2023), which reported Ophiocarpine, Lidocaine, Butyl isobutyl phthalate, and 1,1,3-Triethoxypropane as major bioactive constituents.

Docking analysis revealed that all four ligands interacted with specific amino acid residues within the protein structure (Fig. 18). The calculated binding energies ranged from − 1.88 to − 3.6 kcal/mol (Table 5). Among the tested ligands, Lidocaine exhibited the highest binding affinity (− 3.6 kcal/mol), interacting with Threonine-221 and residue 215. Ophiocarpine formed interactions with multiple residues, including Serine-87, Serine-128, Serine-195,

Table 4 Comparative study of bioflocculant with conventional chemical flocculants

Flocculants	Flocculation of *Microcystis aeruginosa* (%)	Biodegradability/toxicity	Key feature/mechanism	Reference
Ferric chloride	85.42%	Low biodegradability	Chemical coagulant, rapid removal	Taghavijeloudar et al. (2024)
Alum	95.12%	Produce chemical residues	High efficiency	Qi et al. (2020a, b)
Polyethyleneimine	82.10%	Potential toxicity	-	Chen et al. (2018)
Polyacrylamide	92.5%	Synthetic polymer are toxic to environment	Fast flocculation but metal-based coagulant	Li et al. (2020)
Iron oxide immobilized bioflocculant (AJ3)	96.4%	Biodegradable and non-toxic	Bioflocculant-immobilized with Fe_3O_4 nanoparticle	

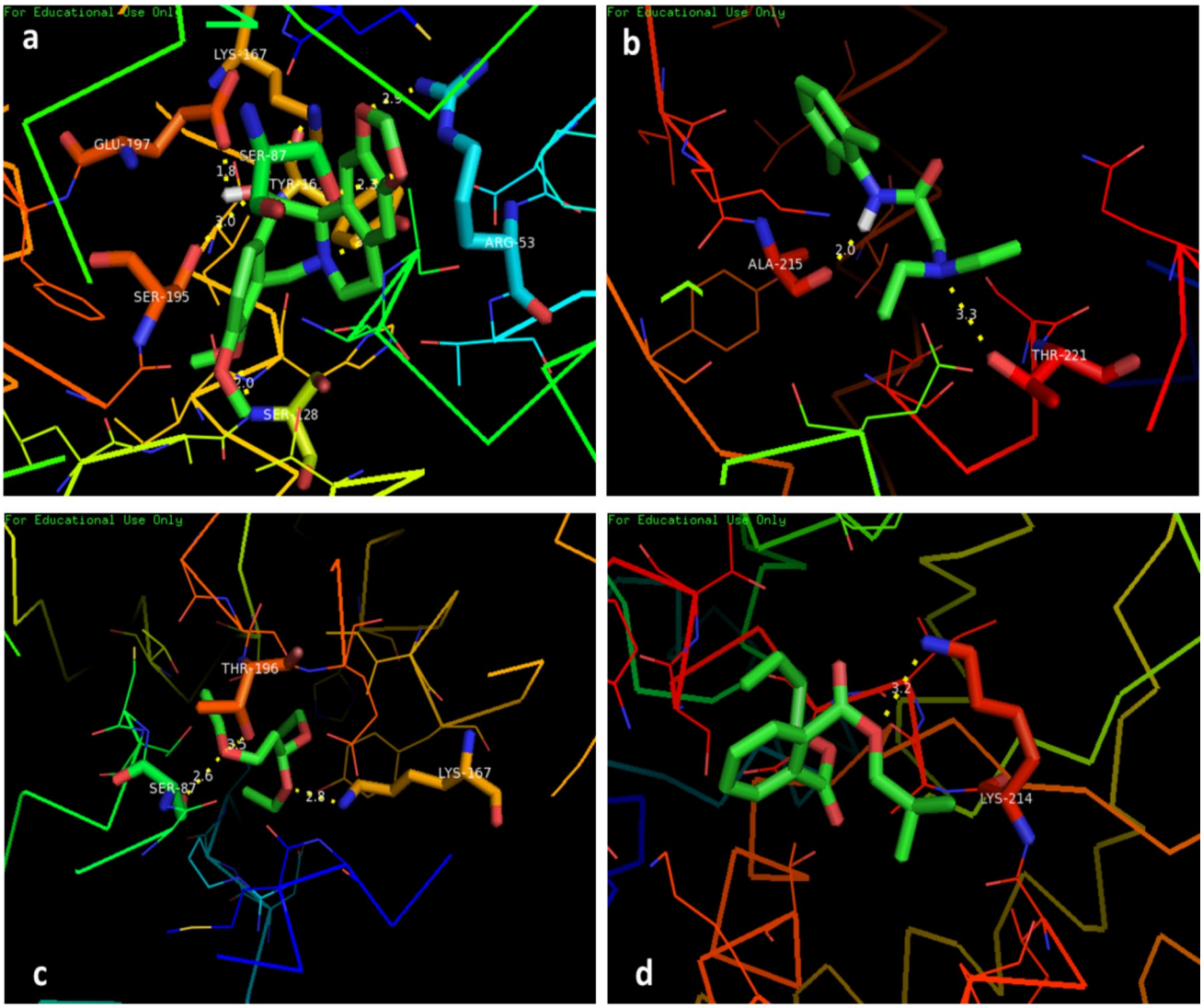

Fig. 18 Molecular docking interactions of bioflocculant-derived compounds with the target protein of *Microcystis aeruginosa* PCC7806: **a** Ophiocarpine; **b** Lidocaine; **c** Butyl isobutyl phthalate; and **d** 1,1,3-Triethoxypropane. Hydrogen bonds and interacting amino acid residues are indicated

Glutamic acid-197, Lysine-167, Tyrosine-163, and Arginine-53, indicating broader surface contact and potential stabilization through hydrogen bonding and electrostatic interactions. Butyl isobutyl phthalate and 1,1,3-Triethoxypropane also demonstrated moderate binding affinities (− 2.67 and − 2.97 kcal/mol, respectively), interacting primarily with Lysine and Threonine residues. The presence of hydrogen bonds and polar interactions suggests that electrostatic attraction and molecular bridging may contribute to the flocculation mechanism. The docking results support the hypothesis that bioflocculant compounds interact with surface-exposed protein residues of *Microcystis aeruginosa*, potentially facilitating aggregation through electrostatic neutralization and bridging interactions. However, the relatively moderate binding energy values indicate that flocculation is likely driven by a combination of multiple weak molecular interactions rather than strong specific ligand–protein binding alone.

Conclusions

A magnetic flocculant synthesized using magnetic Fe_3O_4 particles and bioflocculant AJ3 was developed for efficient *Microcystis aeruginosa* removal. A flocculation efficiency of above 96% was obtained at a dosage concentration of 30 mg/L, pH of 6.5, 37 °C temperature, 120 rpm, and 60 min of settling time to treat the *Microcystis aeruginosa*.

Table 5 Molecular docking of ligands interacts with amino acids and binding energy

S. No.	Name of the ligand/PubChem ID	Binding energy	Interacting amino acids	No. of H-bonds
1	Ophiocarpine	− 1.88	Serine-87 Serine-128 Serine-195 Glutamic acid-197 Lysine-167 Tyrosine 163 Arginine-53	1
2	Lidocaine	− 3.6	alpha-Linolenic acid-215 Threonine-221	1
3	Butyl isobutyl phthalate	− 2.67		Lysine-214
4	1,1,3-Triethoxypropane	− 2.97	Threonine-196 Lysine-167 Serine-87	0

Nanoparticles immobilized with bioflocculants were characterized and optimized under different conditions to measure the flocculation efficacy. Following this, the *Microcystis aeruginosa* was cultivated under optimized conditions and biomass was evaluated. The immobilized bioflocculant Fe_3O_4 nanoparticle flocculation efficacy was revealed to be reusable multiple times, and it reduces the cost. The flocculation mechanism between Fe_3O_4–bioflocculant and *Microcystis aeruginosa* involves an adsorption and bridging mechanism that adsorbs the microalgal cells. Moreover, the docking studies divulge binding energy and binding sites on the targeted microalgal cells. The flocculation efficiency of the immobilized bioflocculant was compared with commercially available flocculants, suggesting that the iron oxide nanoparticle immobilized bioflocculant has greater flocculating activity than commercial flocculants. In addition, antibacterial activity was examined against water pathogenic bacteria of *E. coli*, *Salmonella*, and *Shigella*, showing bacterial activity. Even though a low dosage of flocculant is sufficient for maximum flocculation efficiency, it can also be reused multiple times.

Acknowledgements The authors acknowledge Tamil Nadu State Council for Science and Technology (TNSCST) under Research Funding for Research Scholars (RFRS/TNSCST/RFRS/VR/05/2019-20), Chennai. We are also thankful to the Department of Science Technology (DST), New Delhi, for their financial assistance and Fund for Improvement of S&T Infrastructure (FIST) scheme. We would like to express our sincere thanks to the PG and Research Department of Microbiology, PSG College of Arts and Science, Coimbatore, Tamil Nadu, India. The authors further acknowledge the infrastructure support provided through ICSSR, DST-FIST, and DST/CURIE-PG/2023/24.

Author contributions Jayaprakash Arulraj: conceptualization, methodology, investigation, and writing—original draft. Vino Udappusamy: data curation, formal analysis, and validation; Priya Sundararajan: software, visualization, and writing—review and editing; Shalini Ganeshan: resources and investigation; Nirmal Kumar Ramasamy: supervision and project administration; Revathy Soundararajan: validation and data curation; Embranahalli Mani Rajesh: resources and formal analysis; Gayathri Kaliyannan: funding acquisition, supervision, and writing—review and editing.

Funding This research was supported by the Research Funding for Research Scholars (RFRS/TNSCST/RFRS/VR/05/2019-20), Chennai, Tamil Nadu, India.

Data availability All data is available under request.

Declarations

Ethics approval Not applicable.

Consent to participate Not applicable.

Consent for publication Not applicable.

Competing interests The authors declare no competing interests.

References

Abbasi BA, Iqbal J, Zahra SA, Shahbaz A, Kanwal S, Rabbani A, Mahmood T (2020) Bioinspired synthesis and activity characterization of iron oxide nanoparticles made using *Rhamnus triquetra* leaf extract. Mater Res Express 6(12):1250e7

Agunbiade M, Pohl C, Ashafa O (2018) Bioflocculant production from *Streptomyces platensis* and its potential for river and wastewater treatment. Braz J Microbiol 49(4):731–741

Ajith MP, Aswathi M, Priyadarshini E, Rajamani P (2021) Recent innovations of nanotechnology in water treatment: a comprehensive review. Bioresour Technol 342:126000

Arularasu MV, Harb M, Sundaram R (2020) Synthesis and characterization of cellulose/TiO_2 nanocomposite: evaluation of *in vitro* antibacterial and *in silico* molecular docking studies. Carbohydr Polym 249:116868

Besenhard MO, LaGrow AP, Hodzic A, Kriechbaum M, Panariello L, Bais G, Gavriilidis A (2020) Co-precipitation synthesis of stable iron oxide nanoparticles with NaOH: new insights and continuous production via flow chemistry. Chem Eng J 399:125740

Bisht V, Lal B (2019) Exploration of performance kinetics and mechanism of action of a potential novel bioflocculant BF-VB2 on clay and dye wastewater flocculation. Front Microbiol 10:1288

Bleeke F, Milas M, Winckelmann D, Klöck G (2015) Optimization of freshwater microalgal biomass harvest using polymeric flocculants. Int Aquat Res 7(3):235–244

Dlamini NG, Basson AK, Pullabhotla RV (2020) Wastewater treatment by a polymeric bioflocculant and iron nanoparticles synthesized from a bioflocculant. Polymers 12(7):1618

Fan J, Chen D, Li N, Xu Q, Li H, He J, Lu J (2018) Adsorption and biodegradation of dye in wastewater with Fe_3O_4@MIL-100(Fe) core–shell bio-nanocomposites. Chemosphere 191:315–323

Fraga-García P, Kubbutat P, Brammen M, Schwaminger S, Berensmeier S (2018) Bare iron oxide nanoparticles for magnetic harvesting of microalgae: from interaction behavior to process realization. Nanomaterials 8(5):292

Govarthanan M, Jeon CH, Jeon YH, Kwon JH, Bae H, Kim W (2020) Non-toxic nano approach for wastewater treatment using *Chlorella vulgaris* exopolysaccharides immobilized in iron-magnetic nanoparticles. Int J Biol Macromol 162:1241–1249

Govindhan P, Pragathiswaran C, Chinnadurai M (2018) A magnetic Fe_3O_4 decorated TiO_2 nanoparticles application for photocatalytic degradation of methylene blue (MB) under direct sunlight irradiation. J Mater Sci Mater Electron 29(8):6458–6469

Idris A, Suzana W (2006) Effect of sodium alginate concentration, bead diameter, initial pH and temperature on lactic acid production from pineapple waste using immobilized *Lactobacillus delbrueckii*. Process Biochem 41(5):1117–1123

Jabbar KQ, Barzinjy AA, Hamad SM (2022) Iron oxide nanoparticles: preparation methods, functions, adsorption and coagulation/flocculation in wastewater treatment. Environ Nanotechnol Monit Manag 17:100661

Jayaprakash A, Revathy S, Raj KA, Rajesh EM (2023) Production and characterization of bioflocculant produced by *Bacillus subtilis* OL818309 and its flocculating effect on harmful algae. Res J Biotechnol 18:72–85

Jeong D, Kim DH, Kang IB, Kim H, Song KY, Kim HS, Seo KH (2017) Characterization and antibacterial activity of a novel exopolysaccharide produced by *Lactobacillus kefiranofaciens* DN1 isolated from kefir. Food Control 78:436–442

Justin C, Philip SA, Samrot AV (2017) Synthesis and characterization of superparamagnetic iron oxide nanoparticles (SPIONs) and utilization of SPIONs in X-ray imaging. Appl Nanosci 7(7):463–475

Karpagavinayagam P, Vedhi C (2019) Green synthesis of iron oxide nanoparticles using *Avicennia marina* flower extract. Vacuum 160:286–292

Kesheri M, Kanchan S, Sinha RP (2021) Isolation and *in silico* analysis of antioxidants in response to temporal variations in the cyanobacterium *Oscillatoria sp.*. Gene Rep 23:101023

Kesheri M, Kanchan S, Sinha RP (2022) Responses of antioxidants for resilience to temporal variations in the cyanobacterium *Microcystis aeruginosa*. S Afr J Bot 148:190–199

Khan S, Naushad M, Iqbal J, Bathula C, Sharma G (2022) Production and harvesting of microalgae and an efficient operational approach to biofuel production for a sustainable environment. Fuel 311:122543

Khatun R, Mamun MSA, Islam S, Khatun N, Hakim M, Hossain MS, Barai HR (2022) Phytochemical-assisted synthesis of Fe_3O_4 nanoparticles and evaluation of their catalytic activity. Micromachines 13(12):2077

Kurniawan SB, Imron MF, Sługocki Ł, Nowakowski K, Ahmad A, Najiya D, Hasan HA (2022) Assessing the effect of multiple variables on the production of bioflocculant by *Serratia marcescens*: flocculating activity, kinetics, toxicity, and flocculation mechanism. Sci Total Environ 836:155564

Li H, Wu S, Du C, Zhong Y, Yang C (2020) Preparation, performances, and mechanisms of microbial flocculants for wastewater treatment. Int J Environ Res Public Health 17(4):1360

Li T, Hu J, Zhu L (2021) Self-flocculation as an efficient method to harvest microalgae: a mini-review. Water 13(18):2585

Li Y, Xu Y, Song R, Tian C, Liu L, Zheng T, Wang H (2018) Flocculation characteristics of a bioflocculant produced by the actinomycete *Streptomyces* sp. hsn06 on microalgae biomass. BMC Biotechnol 18(1):58

Lucena MDA, Ramos IFDS, Geronço MS, de Araújo R, da Silva Filho FL, da Silva LMLR, da Costa MP (2022) Biopolymer from water kefir as a potential clean-label ingredient for health applications: evaluation of new properties. Molecules 27(12):3895

Maliehe TS, Selepe NT, Ntombela G, Simonis J, Basson AK, Ngema S, Mpanza F (2016) Production and characteristics of bioflocculant TPT-1 from a consortium of *Bacillus pumilus* JX860616 and *Alcaligenes faecalis* HCB2. Afr J Microbiol Res 10(37):1561–1575

Mallika S, Umamaheswari R, Krishnamoorthy S (2017) Physicochemical parameters and bacteriological study of Vaigai River water, Madurai district, Tamil Nadu, India. Int J Fish Aquat Stud 5(1):42–45

Manivasagan P, Kang KH, Kim DG, Kim SK (2015) Production of polysaccharide-based bioflocculant for the synthesis of silver nanoparticles by *Streptomyces* sp. Int J Biol Macromol 77:159–167

Markeb AA, Llimós-Turet J, Ferrer I, Blánquez P, Alonso A, Sánchez A, Font X (2019) The use of magnetic iron oxide-based nanoparticles to improve microalgae harvesting in real wastewater. Water Res 159:490–500

Mushtaq N, Singh DV, Bhat RA, Dervash MA, Hameed OB (2019) Freshwater contamination: sources and hazards to aquatic biota. Fresh water pollution dynamics and remediation. Springer, Singapore, pp 27–50

Muthulakshmi L, Nellaiah H, Kathiresan T, Rajini N, Christopher F (2017) Identification and production of bioflocculants by *Enterobacter* sp. and *Bacillus* sp. and their characterization studies. Prep Biochem Biotechnol 47(5):458–467

Okaiyeto K, Nwodo UU, Okoli SA, Mabinya LV, Okoh AI (2016) Implications for public health demands alternatives to inorganic and synthetic flocculants: bioflocculants as important candidates. Microbiol Open 5(2):177–211

Prodan AM, Iconaru SL, Ciobanu CS, Chifiriuc MC, Stoicea M, Predoi D (2013) Iron oxide magnetic nanoparticles: characterization and toxicity evaluation by *in vitro* and *in vivo* assays. J Nanomater 2013(1):587021

Pu L, Zeng YJ, Xu P, Li FZ, Zong MH, Yang JG, Lou WY (2020) Using a novel polysaccharide BM2 produced by *Bacillus megaterium* strain PL8 as an efficient bioflocculant for wastewater treatment. Int J Biol Macromol 162:374–384

Qi J, Lan H, Liu R, Liu H, Qu J (2020a) Efficient *Microcystis aeruginosa* removal by moderate photocatalysis-enhanced coagulation with magnetic Zn-doped Fe_3O_4 particles. Water Res 171:115448

Qi X, Zheng Y, Tang N, Zhou J, Sun S (2020b) Bioconversion of citrus peel wastes into bioflocculants and their application in the removal of microcystins. Sci Total Environ 715:136885

Ren B, Weitzel KA, Duan X, Nadagouda MN, Dionysiou DD (2022) A comprehensive review on algae removal and control by coagulation-based processes: mechanism, material, and application. Sep Purif Technol 293:121106

Selepe TN, Akanbi R, Maliehe TS, Moganedi K, Masoko P (2022) Flocculating activity of a bioflocculant from *Bacillus megaterium* BMBF in treatment of domestic and coal mine wastewater. Appl Sci Basel 12(16):8312

Seo JY, Lee K, Lee SY, Jeon SG, Na JG, Oh YK, Park SB (2014) Effect of barium ferrite particle size on detachment efficiency in magnetophoretic harvesting of oleaginous *Chlorella sp.*. Bioresour Technol 152:562–566

Solomon NO, Kanchan S, Kesheri M (2024) Nanoparticles as detoxifiers for industrial wastewater. Water Air Soil Pollut 235(3):214

Stolyar SV, Krasitskaya VV, Frank LA, Yaroslavtsev RN, Chekanova LA, Gerasimova YV, Velikanov DA (2021) Polysaccharide-coated iron oxide nanoparticles: synthesis, properties, surface modification. Mater Lett 284:128920

Taghavijeloudar M, Shabanizadeh H, Yaqoubnejad P, Safaei M (2024) Efficient microalgae harvesting toward biofuel production using a novel plant-based flocculant as a promising alternative to conventional flocculants. Algal Res 81:103557

Udappusamy V, Thinagaran R, Mayakrishnan V, Balakarthikeyan J, Kannappan P, Al-Ghamdi S, Ramesh T (2025) An integrated *in vitro* and *in silico* approach to assess targeted cytotoxicity against MDA-MB-231 triple-negative breast cancer cells with *Psidium guajava* peel-derived chitosan nanoparticles. Artif Cells Nanomed Biotechnol 53(1):43–55

Vélez E, Campillo GE, Morales G, Hincapié C, Osorio J, Arnache O, Jaramillo F (2016) Mercury removal in wastewater by iron oxide nanoparticles. J Phys Conf Ser 687(1):012050

Vergini S, Aravantinou AF, Manariotis ID (2016) Harvesting of freshwater and marine microalgae by common flocculants and magnetic microparticles. J Appl Phycol 28(2):1041–1049

Wang X, Zhao Y, Jiang X, Liu L, Li X, Li H, Liang W (2018) *In situ* self-assembly of plant polyphenol-coated Fe_3O_4 particles for oleaginous microalgae harvesting. J Environ Manag 214:335–345

Xia M, Zhou H, Amanze C, Hu L, Shen L, Yu R, Zeng W (2022) A novel polysaccharide-based bioflocculant produced by *Bacillus subtilis* ZHX3 and its application in the treatment of multiple pollutants. Chemosphere 289:133185

Zhang D, Ye Q, Zhang F, Shao X, Fan Y, Zhu X, Xu H (2019) Flocculating properties and potential of *Halobacillus* sp. strain H9 for the mitigation of *Microcystis aeruginosa* blooms. Chemosphere 218:138–146

Zhang W, Liu J, Xiao Y, Zhang Y, Yu Y, Zheng Z, Li Q (2022) The impact of cyanobacteria blooms on the aquatic environment and human health. Toxins 14(10):658

Zhao Y, Liang W, Liu L, Li F, Fan Q, Sun X (2015) Harvesting *Chlorella vulgaris* by magnetic flocculation using Fe_3O_4 coating with polyaluminium chloride and polyacrylamide. Bioresour Technol 198:789–796

Zou X, Li Y, Xu K, Wen H, Shen Z, Ren X (2018) Microalgae harvesting by buoy-bead flotation process using bioflocculant as alternative to chemical flocculant. Algal Res 32:233–240